Petrology, Vol. 12, No. 6, 2004, pp. 561–582. Translated from Petrologiya, Vol. 12, No. 6, 2004, pp. 632–655.

Dispersed Mafic–Ultramafic Intrusive Magmatism in Early Paleoproterozoic Mobile Zones of the Baltic Shield: An Example of the Belomorian Drusite (Coronite) Complex

E. V. Sharkov, I. S. Krassivskaya, and A. V. Chistyakov

Institute of the Geology of Ore Deposits, Petrography, Mineralogy, and Geochemistry (IGEM), Russian Academy of Sciences, Staromonetnyi per. 35, Moscow, 119017 Russia
e-mail: sharkov@igem.ru

Received November 18, 2003

Abstract—The Early Paleoproterozoic (2.46–2.36 Ga) Belomorian drusite (coronite) complex was addressed to for the first time in discussing the geology, petrology, and genesis of dispersed intrusive mafic–ultramafic magmatism that developed between cratons and granulite belts of Early Precambrian age. The complex comprises numerous small rootless synkinematic intrusions that are scattered throughout the Belomorian Mobile Belt (BMB). The rocks of the complex are compositionally close to the rocks of large layered intrusions in the neighboring cratons and compose, together with them, the Baltic Large Igneous Province (BLIP) of the silicic high-Mg (boninite-like) series. It is demonstrated that the magma generation regions were similar beneath the cratons and BMB, but, in contrast to the situation at the cratons, melt portions ascending from below the BMB could be accommodated only in small chambers, whose position was controlled by local heterogeneities induced by the tectonic flowage of the host rocks. Moreover, these chambers continuously changed their position, thus precluding the origin of large bodies and eventually giving rise to dispersed magmatism. Upon their crystallization, the intrusions were affected by tectonometamorphic reworking under amphibolite-facies conditions, so that relatively little altered rocks are now preserved only in the cores of these bodies. The rocks are characterized by the development of drusite (coronite) textures along the grain boundaries of primary magmatic minerals.

INTRODUCTION

The principal Early Paleoproterozoic tectonic structures of the Baltic Shield were rigid Archean Karelian and Kola cratons, which were separated by the Lapland–Umba Granulite Belt (LUGB) (Fig. 1). Its boundaries with neighboring cratons were marked by the development of intercratonic mobile belts: Belomorian (BMB) in the southwest and Tersk–Lotta (TLMB) in the northeast (Sharkov *et al.*, 2000). The cratons were uplifted extending areas with mantle-related magmatism, whereas LUGB was a compressed subsiding compensation structure with crustal synkinematic enderbite–charnockite magmatism. The mobile belts in between were zones of low-angle tectonic flowage in an extensional environment. These zones were composed mostly of tectonic slabs of Archean rocks detached from the neighboring cratons.

For the purposes of our research, it is most interesting to trace correlations between magmatic processes that occurred simultaneously in different tectonic environments: (i) in rigid cratons and (ii) transitional mobile belts in the Baltic Shield. In both situations, these processes produced silicic high-Mg (boninite-like) series (SHMS) of mantle-crustal origin, which are compositionally close to Phanerozoic island-arc series but were derived in a principally different tectonic environment (Sharkov *et al.*, 1997). The SHMS rocks are components of the Baltic Large Igneous Province (BLIP), which was dated at 2.55–2.36 Ga (Sharkov *et al.*, 1997), but the character of the processes in these environments was principally different. In cratons, they generated large mafic–ultramafic layered intrusions, dike swarms, and volcanosedimentary complexes in riftogenic structures (Pechenga–Varzuga, Vetreny Belt, and others). Conversely, in intercratonic mobile belts, these processes gave rise mostly to numerous small synkinematic intrusions of mafic and ultramafic rocks disseminated throughout the area of the belts.

Within the BMB, these bodies are always variably metamorphosed and transformed into so-called drusites (this local term was coined by E.S. Fedorov in 1905 to denote coronitic metagabbro). In the course of regional metamorphism, reactions between the mafic magmatic minerals of these rocks and their plagioclase produced concentric rims of metamorphic minerals (mostly clinopyroxene, hornblende, and garnet). The drusite complex includes, along gabbro, numerous coronitic mafic–ultramafic rocks, all of which were collectively referred to as *drusites* and were thoroughly studied by many geologists and petrologists, among whom we would like to mention N.G. Sudovikov, K.A. Shurkin, G.M. Saranchina, L.A. Kosoi, V.L. Duk, F.P. Mitrofanov, M.M. Efimov,

N.D. Malov, V.S. Stepanov, A.I. Slabunov, and many others.

Petrological analysis demonstrates that phase equilibria in the coronites, the chemistry of their metamorphic clinopyroxene and garnet, and the *P–T* metamorphic parameters are absolutely identical to the analogous values characteristic of the Karelian (Svecofennian) prograde metamorphism (at 1.9 Ga) in the host garnet–clinopyroxene amphibolites (Larikova, 2000; Korikovsky, 2004) and were $T = 650–700°C$ at $P > 6$ kbar (Larikova, 2000). The pressure value was lately refined by Korikovsky (2004) at 9–10 kbar.

For the purposes of this publication, it is important to stress that the coronitization of the gabbro and ultramafics comagmatic with it was apparently isochemical, when magmatic textures and relics of magmatic olivine, orthopyroxene, and plagioclase, as well as magmatic structures, such as layering, etc., remain well reserved in spite of the wide spreading of both embryonic and well-developed orthopyroxene, clinopyroxene, and garnet reaction rims. All of the petro- and geochemical samples used in this research were taken from massive, mostly coronitized rocks without petrological traces of overprinted metasomatism and component migration. Because of this, it is assumed that all geochemical characteristics of the mafic–ultramafic complex correspond to its primary magmatic nature.

In contrast to magmatism in cratons, which was studied fairly thoroughly, the dispersed magmatism of intercratonic mobile belts remains known inadequately poorly. It is pertinent to emphasize that drusite magmatism is one of the principal discriminators of the tectonic environment and boundaries of the BMB, because cratons contain vast swarms of dikes of the same age and composition. At the same time, these processes are a specific manifestation of endogenic activity, whose understanding provides better insight into the distinctive features of Precambrian tectono-magmatic processes. Inasmuch as this paper is devoted to the magmatic (pre-coronite) history of the mafic rocks, below we will omit the adjectives *coronitic* or *drusitic* and name the respective rocks according to their primary magmatic nature, with the prefix *meta-* attached only to the names of strongly altered petrographic varieties.

GEOLOGY OF THE BELOMORIAN CORONITE COMPLEX

The mafic–ultramafic coronite complex comprises multiple small (from a few hundred meters to 1–2 km long or, rarely, larger) bodies, which range from tens to hundreds of meters in thickness. These are rootless mafic and ultramafic (more rarely, intermediate) intrusions, which are abundant among high-grade metamorphic rocks of the BMB. The intrusions are dominated by norite and gabbronorite bodies with subordinate amounts of ultramafics (plagioclase harzburgites, bronzitites, websterites, and predominant plagioclase lherzolites), anorthosites, and magnetite gabbrodiorites. The total number of the intrusions amounts to tens of thousands (Malov and Sharkov, 1978). The relative abundances of different rock types in the complex, calculated over an area of about 6000 km^2 in northern Karelia by N.D. Malov and refined during later studies, are as follows: ~16% ultramafics, 30% olivine norites and gabbronorites, 30% norites and gabbronorites, 20% for gabbronorite-anorthosites and anorthosites, and ~4% magnetite gabbro-diorites and diorites. This roughly corresponds to the abundances of the same rock types in large mafic–ultramafic intrusion (Monchegorsk, Burakovsky, Koilismaa, and others) in the neighboring cratons. However, these rocks in the BMB are obviously prone to form individual bodies.

An analogous style of Early Paleoproterozoic magmatic activity is typical of the coeval Tersk–Lotta Mobile Belt. This belt also includes numerous small synkinematic bodies of mafic and ultramafic rocks, which are most typical of the Monchegorsk district (Kozlov *et al.*, 1967) and the southern foothills of the Chuna-Tundra Range (Mitrofanov and Pozhilenko, 1991).

In both belts, the most widespread bodies consist of a single rock type. These bodies usually have the shapes of distorted ovals, often with tectonic contacts and marginal parts metamorphosed to the amphibolite facies and with relatively little altered rocks usually preserved in their cores. Primary intrusive contacts are much more rare.

Judging by the best preserved bodies of the complex, they could originally be sills or dikes or have the morphologies of irregular lenses and, in places, horseshoes (in map view), filling the detachment space in the hinges of relatively large folds (Fig. 2). This provides grounds to hypothesize that the melt was emplaced simultaneously with deformations of the host rock, which is consistent with the results of the statistical studying of the distribution of Belomorian drusite intrusions (Malov and Sharkov, 1978). These bodies were determined to definite group along permeable zones (Fig. 3), which coincide with the predominant orientation of deformations in the Early Paleoproterozoic (Volodichev, 1990).

SOME EXAMPLES OF THE STRUCTURES OF THE MAFIC–ULTRAMAFIC BODIES

According to their composition, the intrusions are subdivided into two major types: (1) predominantly mafic (gabbronorite-anorthosite) and (2) predominantly ultramafic (lherzolite–gabbronorite). Their examples will be presented below. Generally, the distribution of drusite bodies according to their composition shows no clear zoning: as can be seen from Fig. 1, even an area in Pezhostrov Island contains virtually all rock types, a feature characteristic of the whole Belomorie

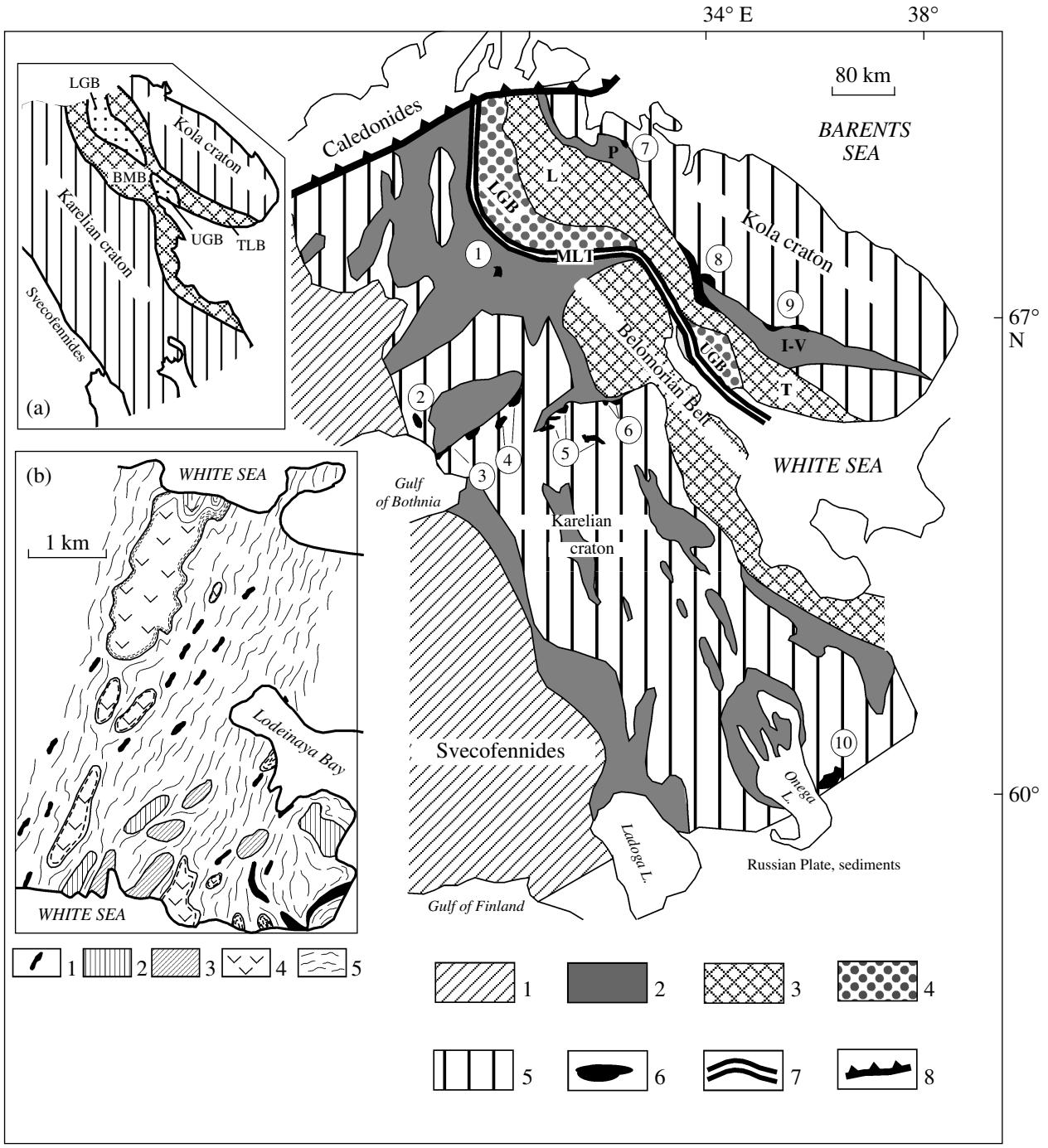

Fig. 1. Early Paleoproterozoic Baltic large igneous SHMS province (after Sharkov *et al.*, 1997). (1) Svecofennides; (2) Paleoproterozoic sedimentary-volcanic complexes (P—Pechenga. I–V—Imandra–Varzuga); (3) intercratonic mobile belts (BMB—Belomorian, TLMB—Tersk–Lotta: L—Lotta and T—Tersk segments); (4) granulite belts (LGB—Lapland and UGB—Umba); (5) Archean basement; (6) layered intrusions (circled numbers: 1—Koitilainen, 2—Tornio, 3—Kemi, 4—Penikat, 5—Koilismaa, 6—Olanga (Oulanka) group, 7—Mt. General'skaya, 8—Moncha Tundra, 9—Fedorovo–Pana, 10—Burakovsky); (7) Main Lapland Thrust (MLT); (8) northern boundary of the Baltic Shield.

Insets: (a) Position of major structural domains in the eastern part of the Baltic Shield in Early Paleoproterozoic time Sumian–Sariolian). (b) Schematic geological map of the central part of Pezhostrov Island, Keret' Archipelago, White Sea (prepared by E.V. Sharkov and A.V. Chistyakov). (1) Lens- and dike-shaped bodies of garnet amphibolites; (2) gabbronorite–lherzolite bodies; (3) coarse-grained bodies of strongly altered gabbronorites; (4) metagabbro-anorthosite bodies, dashed lines along the contacts indicate shear and amphibolization zones; (5) host Archean plagiomigmatites.

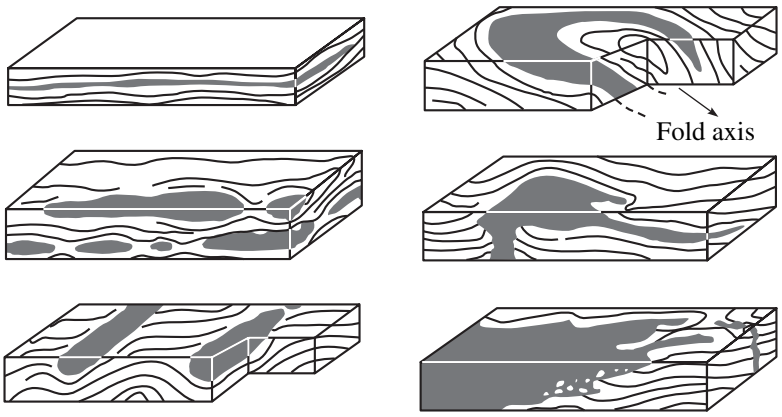

Fig. 2. Morphology of drusite intrusions [after (Shurkin *et al.*, 1962)].

region, in which from one to three intrusions on average are usually exposed within a 1-km^2 area.

Bodies of Mafic Rocks (Gabbronorite-Anorthosite)

The anorthosite body of Pezhostrov Island of the Keret' Archipelago in the White Sea has a roughly rectangular shape ~1 km long and ~200–300 m wide and is elongated nearly northward, conformably with the trends of the host Archean granite-gneisses (Fig. 1). The geology and petrology of this intrusion were described in detail in (Sharkov *et al.*, 1994), and here we present only the most general information. The intrusion is dominated by gabbronorite-anorthosite and contains subordinate amounts of gabbronorite. The southeastern part of the body includes magnetite gabbronorite and gabbrodiorite, which likely correspond to the uppermost part of the body. The contacts between them and the host rocks are always tectonic, except only for the northern part, where fine- to medium-grained leucogabbronorites occur, which seem to compose the inner-contact zone of the intrusion. All of the rocks were extensively deformed and blastomylonitized under amphibolite-facies conditions and are now mostly transformed into plagioclase schists and amphibolites. Their primary magmatic textures and structures are preserved only occasionally. The crystallization of the massif was dated at 2452 ± 20 Ma (zircon U–Pb age); the $^{207}Pb/^{206}Pb$ age of the metamorphic apatite is approximately 1789 Ma (Alexejev *et al.*, 2000).

The blastomylonitization zones cutting across the Pezhostrov body have a complicated morphology and are often intruded by conformable mafic dikes, which are transformed into garnet amphibolites. Chemically, these dikes affiliate with SHMS (Sharkov *et al.*, 1994). The morphology of the dikes, whose material was forced into the hinges of folds, and the absence of these dikes from parts of the intrusion consisting of more massive rocks led us to suggest that they were emplaced simultaneously with blastomylonitization of the already-solid host intrusive rocks. Analogous dikes and boudins of garnet amphibolites occur in the host gneisses (Fig. 1).

The original morphology of the intrusion remains unknown. It could be a fragment of a large lens-shaped body that was affected by many stages of overprinted deformations and metamorphism. These processes disintegrated the body into blocks, which were then pulled apart in the course of the plastic flow of the host migmatites (Fig. 1).

An insight into the character of the primary layering of these bodies is provided by a small metagabbro–anorthosite body in the eastern part of Island Lodeinyi in the Kandalaksha Archipelago. The body is a large lens-shaped boudin in migmatites (Fig. 4). Its western portion consists of mostly massive gabbronorites, and the eastern part is made up of gabbronorite-anorthosites with irregularly shaped thin gabbronorite layers. The layered rocks show sliding structures of the crystalline material, which suggest that the intrusion was emplaced under dynamic conditions.

The strongly altered metagabbro–anorthosite intrusion in the southwestern part of Anisimov Island in the Kandalaksha Archipelago has a length of >1.6 km (the length of the island itself) and a width of at least 200 m (Fig. 5). All contacts of the body with the host Archean granite-gneisses and migmatites are tectonic, through zones of shearing of all rocks, to which younger migmatization is often restricted. Analogous zones divide the intrusion into large blocks: (1) Coarsely layered metagabbronorite-anorthosites with subordinate amounts of gabbronorites and relatively thin (1–3 cm) pyroxenite (websterite) layers. There are traces of the sliding of the crystalline material, as in Lodeinyi Island (Fig. 5, II). (2) Thinly layered rocks with alternating layers of olivine metapyroxenites and metagabbronorites. The layers are 1–2 cm, rarely up to 10 cm, thick (Figs. 5, I and 6a).

These thinly layered rocks include a nearly conformable dike of plagioclase olivine websterite meta-

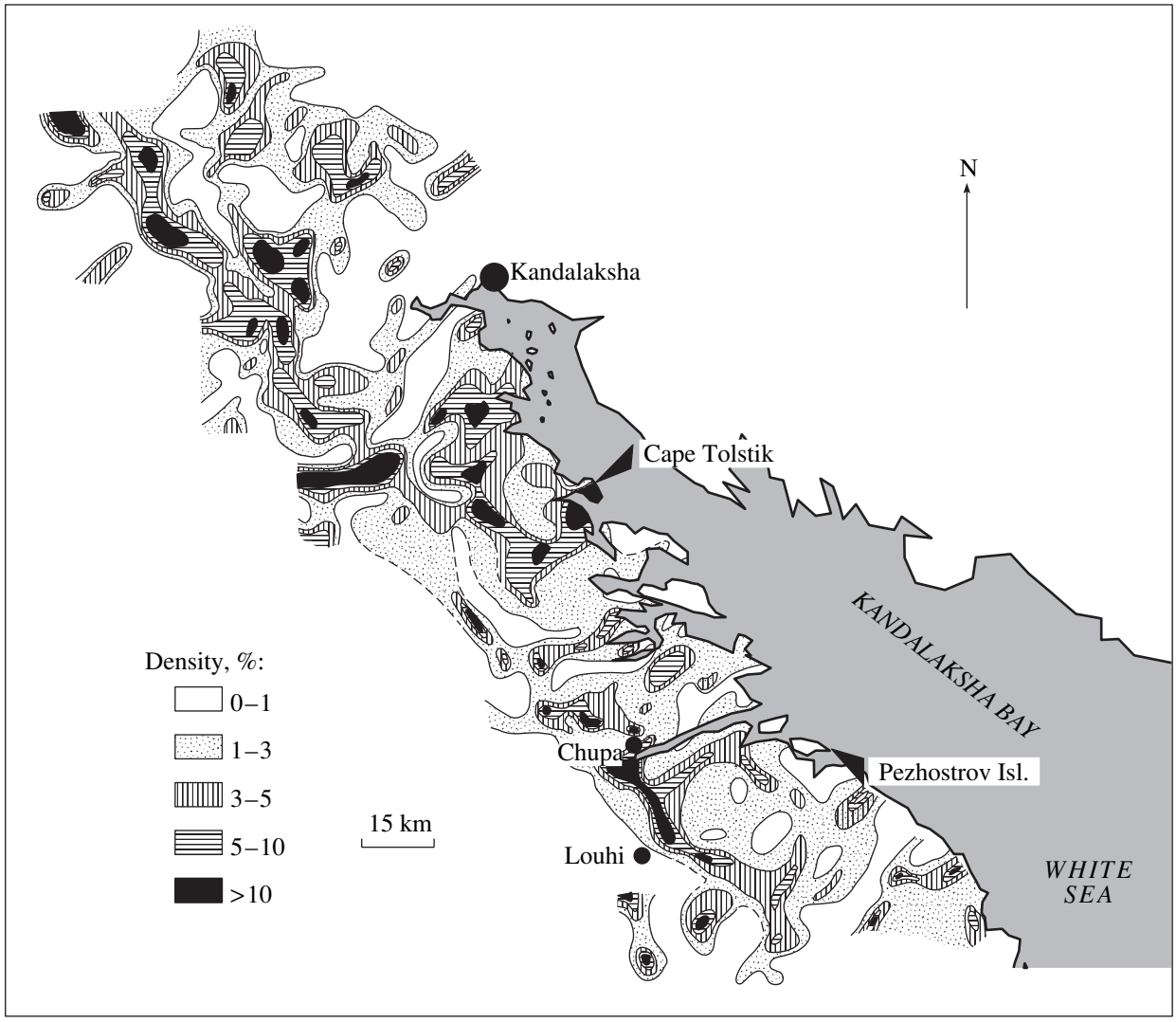

Fig. 3. Schematic map showing the distribution density (percentage of the total area) of drusite massifs in the Belomorian Mobile Belt [modified after (Malov and Sharkov, 1978)].

morphosed to the same metamorphic grade. The primary contacts of the dike have a complicated morphology (Fig. 6b). In contrast the Pezhostrov Massif, this dike was obviously intruded before shearing: as can be seen in Fig. 5, I, the blastomylonite zone cuts across both this dike and the host sheared gabbroids.

Although the blocks of the massif are elongated northwestward (conformably with the general trends of the migmatites), their layering is oriented roughly westward (Fig. 5, I). This suggests that the Anisimov Island intrusion originally trended northward. The modern morphology of its fragments seems to has been caused by its dividing into blocks in the process of the plastic flowage of the host migmatites matrix during later evolutionary stages of the BMB.

Although this massif was not dated, age values were obtained for an analogous body in nearby Voronii Island. The U–Pb isochron zircon age of its crystallization is 2460 ± 10 Ma, and pale rutile from these rocks was dated (by the same method) at 1775 ± 45 Ma (T.B. Bayanova, personal communication), which coincides, within the error, with data on the Pezhostrov anorthosite massif.

The intrusion in Cape Tolstik is located in the western shore of Kandalaksha Bay (Fig. 3). This is a relatively large lens-shaped elongated body approximately 6 km long and 2 km wide, which trends northwestward. It is composed of gabbronorites, gabbronorite-anorthosites, and magnetite gabbronorites, and gabbronorite-diorites (Efimov *et al.*, 1987; Bogdanova, 1996). The intrusion was dated at 2434 ± 7 Ma, the age of the host Archean plagiogneisses is 2741 ± 43 Ma, and the cutting pink potassic granites have an age of 2405 ± 5 Ma (U–Pb data on zircon; Bibikova *et al.*, 1993; Bogdanova, 1996). The contacts of the body are tectonic. The rocks preserve their magmatic textures in the core of the intrusion and are transformed into garnet

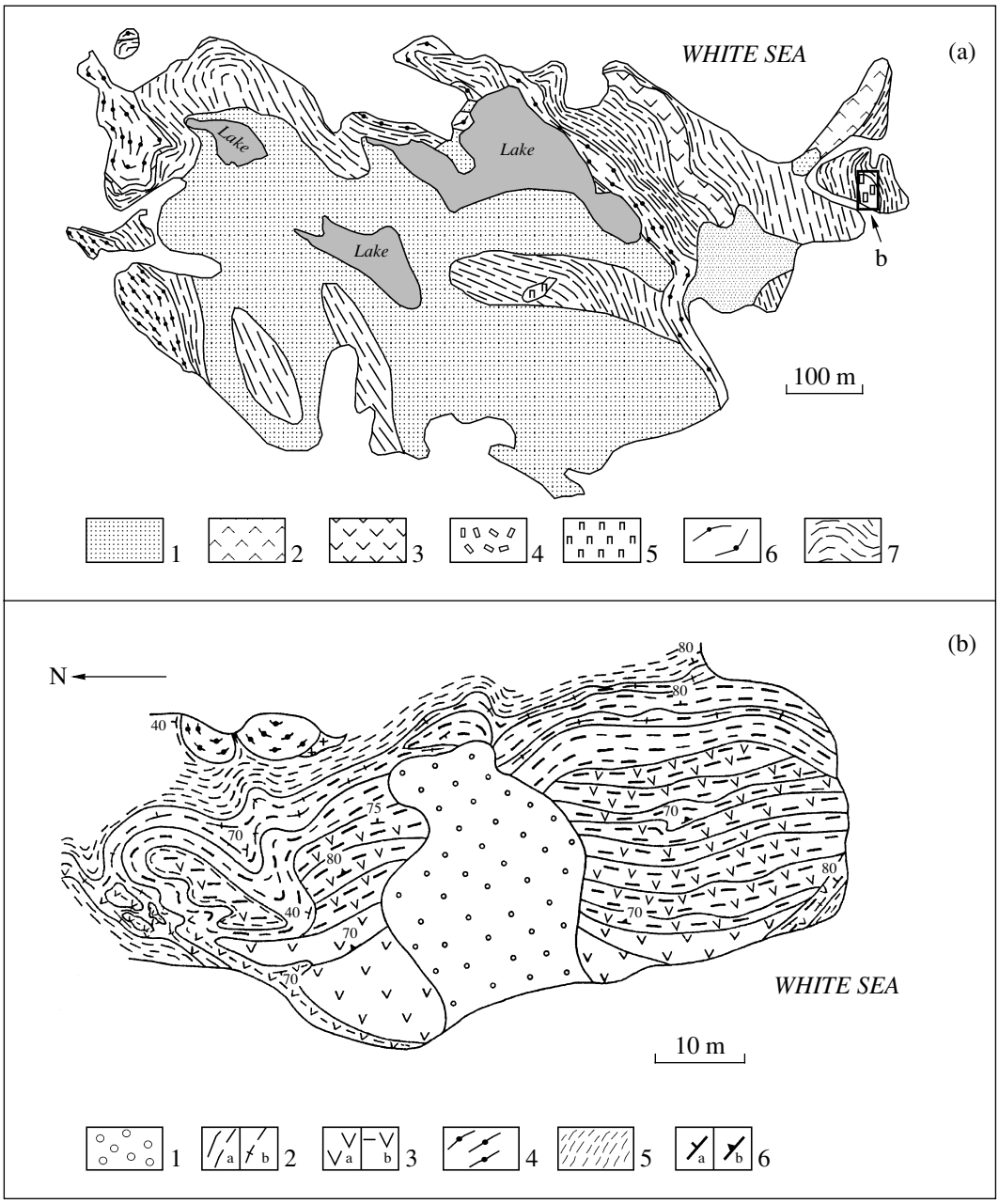

Fig. 4. Bodies of the drusite complex in the Lodeinyi Island, Kandalaksha Archipelago, White Sea (prepared by E.V. Sharkov).
(a) Schematic geological map of the island. (1) Quaternary deposits; (2) gabbronorites and olivine gabbronorites; (3) metagabbronorites; (4) metagabbro-anorthosites; (5) plagioclase lherzolite bodies; (6) garnet amphibolites; (7) migmatites.
(b) Geological structure of the drusite body (block) of layered metagabbro-anorthosites and gabbronorites. (1) Quaternary deposits; (2) (a) garnet amphibolites and (b) amphibolites after gabbronorite-anorthosites; (3) variably altered (a) gabbronorites and (b) gabbronorite-anorthosites with relict magmatic textures and structures; (4) garnet amphibolite boudins; (5) plagiomigmatites; (6) strikes and dips of: (a) migmatites and amphibolites developing after rocks of the drusite complex, (b) primary magmatic layering.

amphibolites and garnet–amphibole gneisses in the margins of the body and along crosscutting shear zones.

The intrusion is cut by at least three generations of mafic dikes. The earliest of them are roughly coeval with the intrusion itself, intermediate dikes are younger than the intrusion but older than the potassic granites, and the youngest dikes cut these granites (Bogdanova, 1996). Analogous dikes were also found in the host rocks. The repeated magma injections (mafic bodies, dikes, and potassic granites) were associated with intense subhorizontal shearing and folding. According to S. Bogdanova, the rocks underwent high-pressure metamorphic transformations before the emplacement of the potassic granites, a process that formed meta-

morphic mineral assemblages (mostly garnet and green hornblende) in the main body and two oldest dike generations. The youngest mafic dikes were affected by regional deformations at 1.9–1.8 Ga (Aleksejev *et al.*, 1999).

Bodies of Ultramafic Rocks (Lherzolite–Gabbronorite)

The lherzolite–gabbronorite intrusions of Pezhostrov Island are a few relatively small bodies in the southern part of the island (Fig. 1), which are hosted by Archean plagiomigmatites. In the Southern Body, 110 by 180 m in size, plagioclase lherzolites grade through olivine gabbronorites to pyroxenites and melanocratic norites. The rocks are mostly massive. Their coarse layering is oriented generally conformably with strike of the body. The contacts of the body are tectonized, and its eastern contact is truncated by a younger migmatization zone 5–10 m thick, which abounds in angular rock fragments from the body that are transformed into amphibolites.

The intrusion of Gorelyi Island is elongated to the northeast (Fig. 7) and has a length of approximately 1 km at a width of 300 m in the broadest part. Similarly to most of the intrusions described above, the initial sizes of the body are unknown, because it extends beneath the White Sea shoreline and is truncated by a fault in the west. The western part of the body is layered, with alternating plagioclase lherzolite and olivine gabbronorite layers from 30 to 50 cm thick, which are generally conformable with the trend of the body. The eastern part of the body, which exhibits an intrusive contact with the host Archean gneisses (Fig. 8), is characterized by fine-grained massive structures and apophyses into the host rocks. The material of the apophyses is usually amphibolized, and primary relict fine-grained gabbronorites with an ophitic texture are preserved only locally. The contact surface is almost vertical with minor deviations.

The lens-shaped body of fine-grained melanocratic metagabbronorites in Lodeinyi Island is elongated to the northeast, conformably with the structure of the host gneisses and migmatites (Fig. 4). Our samples from this intrusion were dated by B.V. Belyatskii (TIMS U–Pb zircon age) on a Finnigan MAT-261 eight-collector mass spectrometer at the Institute of Precambrian Geology and Geochronology, Russian Academy of Sciences. The age of the intrusion was evaluated at 2442 ± 3.6 Ma (Fig. 9).

The primary intrusive contact of this body with the host Archean gneisses principally differs from the contact in Gorelyi Island. The former is marked by a specific rind, approximately 1 m thick, which consists of green hornblende, clinopyroxene, plagioclase, and quartz and contains small (2–3 cm long) partially reworked skialiths of fine-grained gabbroids and host gneisses. The material of this rind grades, on the one hand, into gabbronorite and, on the other, into the host gneiss. The gneiss in the 1.5- to 2-m-thick outer-contact zone is partly recrystallized, its biotite is decomposed (one of the products is orthoclase), and the rock contains newly formed granophyric segregations and becomes more massive. This character of the contact was, perhaps, caused by bimetasomatic processes (like skarn processes), when the already solidified but still hot mafites interacted with the host granites. Obviously, the origin of such a diffusion contact required that the host rocks were heated to higher temperatures than those at the "normal" intrusive contact, such as in Gorelyi Island. Another interpretation (S.P. Korikovsky, personal communication) is the younger migmatization of the gabbroids.

The Yudom-Navolok and Shang intrusions are exposed in the shores of Domashnyaya (Pon'goma) Bay in northern Karelia, 200–250 km south of the Kandalaksha and Keret' archipelagoes. In contrast to many other localities in the White Sea area (Belomorie), this is dominated by north-trending deformations that controlled the emplacement of intrusions of the complex but were not affected by extensive tectono-metamorphic recycling (Stepanov, 1981).

The Yudom-Navolok intrusion is a relatively large body, which trends roughly northward for no less than 5 km and has a width from 80 to 150 m. It is composed of plagioclase lherzolites, pyroxenites, olivine gabbronorites, leucocratic gabbronorites, and granophyric gabbro and gabbronorites. The rare layering is oriented roughly to the north, conformably with the trend of the massif itself. Lherzolites are prone to be restricted to the southern exposures of the massif, which seem to correspond to its lower part.

The intrusive contacts with the host migmatized garnet–biotite gneisses are well exposed and can be observed in many outcrops. These contacts are commonly highly tortuous and complicated with apophyses and embayings, with the contact rocks abounding in xenoliths of the host rocks. The inner-contact zone is 3–5 m thick, consists of fine-grained gabbronorite, and is marked by xenoliths of garnet gneisses and amphibolites. The gabbronorites always contain garnet and amphibole, mostly in the form of discontinuous rims around plagioclase and pyroxene grains or as inclusions in plagioclase.

A distinctive feature of the contact gabbronorites is the presence of granophyric varieties. The chilled-zone gabbroids are cut by veinlets of fine-grained aplitic granite (up to 30–50 cm thick), which extend from the contact with the host gneisses and have undulating but sharp boundaries with small tongues. These veinlets of anatectic granites cut across the chilled facies of the intrusion and xenoliths. The granites commonly bear minor amounts (<5 vol %) of disseminated biotite and small aggregates of garnet grains.

The massif of Shang Island (1 km × 100 m) is a homogeneous body, consisting of massive lherzolites and plagioclase lherzolites. The contacts of the intru-

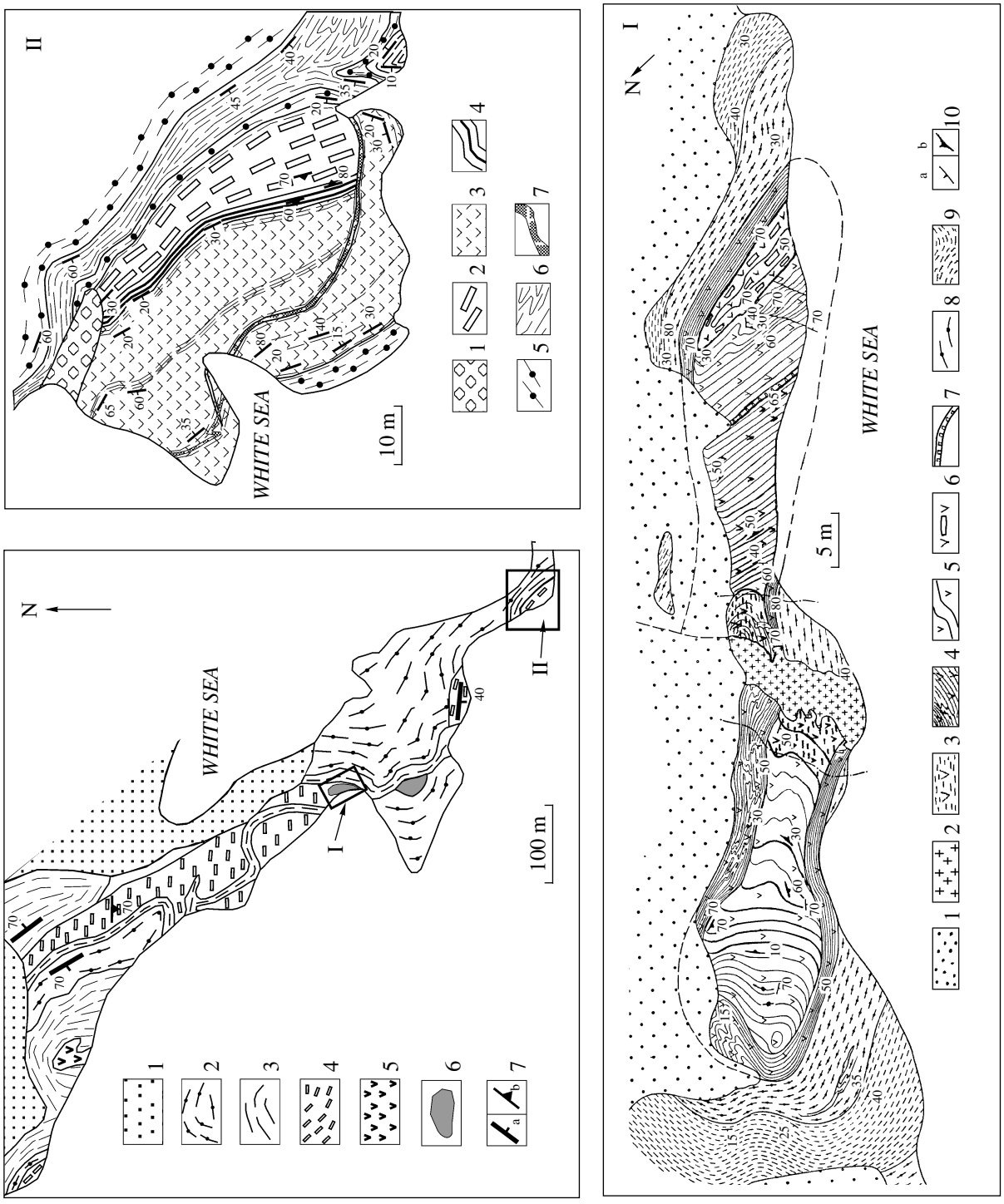
N
WHITE SEA
100 m
I
II
1
2
3
4
5
6
7
II
WHITE SEA
10 m
1
2
3
4
5
6
7
N
I
WHITE SEA
5 m
1
2
3
4
5
6
7
8
9
10

Fig. 5. Schematic geological map of the southern part of Anisimov Island (prepared by E.V. Sharkov) and detailed maps of blocks of (I) thinly layered gabbronorites and (II) leucocratic gabbroids. (1) Quaternary deposits; (2) garnet amphibolites; (3) migmatites; (4) gabbronorite-anorthosites and gabbronorites; (5) garnet gabbro-amphibolite; (6) blocks of thinly layered intrusive rocks; (7) strikes and dips of: (a) gneissosity, (b) primary layering. (I) Detailed map of a block of thinly layered gabbronorites. (1) Quaternary deposits; (2) granite pegmatites; (3) diaphthorized thinly layered gabbroids in contact with a pegmatite vein; (4) garnet amphibolite developing after gabbroids; (5) thinly intercalating gabbronorite and pyroxenites (see Fig. 6a); (6) metagabbronorite-anorthosites; (7) subconformable olivine pyroxenite dike (see Fig. 7); (8) garnet amphibolites; (9) migmatites; (10) strikes and dips of: (a) gneissosity, (b) primary layering. (II) Detailed map of a block of leucocratic gabbroids. (1) Quaternary deposits; (2) gabbronorite-anorthosites; (3) gabbronorites; (4) cyclically intercalating gabbronorites and gabbronorite-anorthosites; (5) garnet amphibolites; (6) migmatites; (7) diabase dike.

sion are concealed beneath the waters of the White Sea. Its northern margin is richer in irregularly shaped lens-like gabbronorite bodies and rare thin segregations and veinlets of pegmatoid.

PETROGRAPHY OF THE COMPLEX

The least altered rocks of the drusite complex are characterized by cumulative magmatic textures, so that their descriptions below will be given within the scope of the terminology currently adopted for cumulate rocks. The chemistry of minerals (their microprobe analyses) are given in Tables 1–4.[1]

As can be seen from our data (Table 1), *Ol* has similar compositions in all of the *Ol*-bearing rocks. The X_{Mg} of the orthopyroxene systematically decreases from En_{81} to En_{65} in the rock sequence from the lherzolites to gabbronorite-anorthosites (Table 2). It should be stressed that the pyroxene compositions (in both the magmatic assemblages and the reaction coronas) define fairly compact fields in a *Wo–En–Fs* diagram (Fig. 10), which are somewhat shifted toward pigeonite-augite or ferrous hypersthene for some massifs.

Plagioclase lherzolites are the most widespread ultramafics of this complex, in which lherzolites are usually described as a series of cumulates from $Ol \pm Chr$ and $Ol + Opx \pm Chr$ to $Ol + Opx + Cpx \pm Chr$ with the predominance of the latter. The intercumulus material can account for 30–35% of these rocks by volume. In the type-I cumulates, it is dominated by *Pl* and contains *Opx* and *Aug*; this material in the type-II cumulates also includes *Pl* and *Aug*, and the type-III cumulates contain plagioclase-dominated intercumulus material. The minor minerals are *Bt*, *Phl*, *Qtz*, and rare *Or* and *Ap*. Formally, the petrography of these rocks corresponds to plagioclase lherzolite. The compositions of mafic minerals vary within fairly broad ranges (mainly from intrusion to intrusion, Tables 1–4).

The interstitial plagioclase of these rocks usually has a dark color due to very fine dust of aluminous spinel, as was determined on a microprobe (Larikova, 2000). Larikova believes that the spinel was produced via the metamorphic decomposition of the anorthite component of plagioclase.

The *olivine gabbronorites* differ from the rocks described above in bearing cumulative plagioclase, which occurs as weakly zonal dusted labradorite laths ($An_{55–68}$ in the cores). The orthopyroxene of these rocks is less magnesian than in the plagioclase lherzolites, whereas the composition of olivine remains the same. The intercumulus pigeonite–augite accounts for 25% of the rocks by volume. The subordinate intercumulus phases are *Or*, *Qtz*, *Bt*, and *Ilm*.

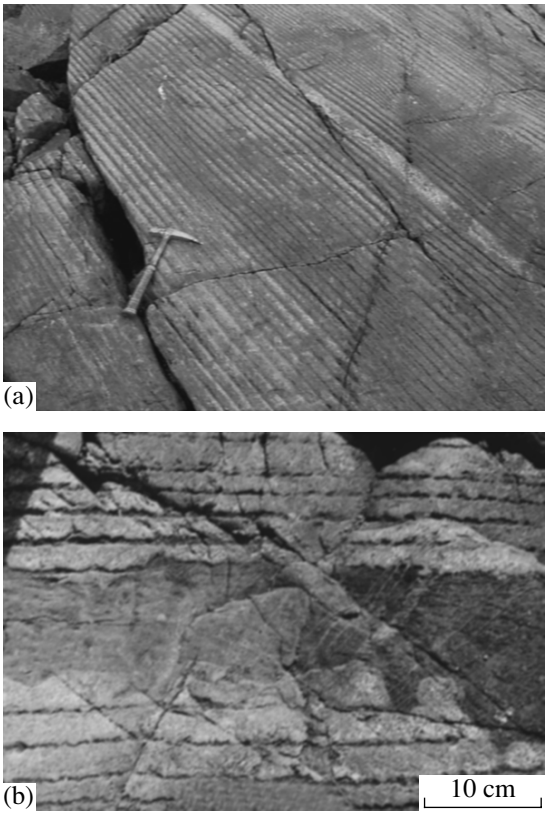

Fig. 6. Thin primary layering in Block I of the Anisomov Island block (see Fig. 5).
(a) Thinly intercalating metagabbronorites and metapyroxenites; (b) Olivine metapyroxenite dike cutting thinly layered gabbronorite, Anisimov Island. Photo: A.V. Chistyakov.

[1] Mineral symbols: *Ol*—olivine, *Opx*—orthopyroxene, *Cpx*—clinopyroxene (*Aug*—augite, *Pig*—pigeonite, *Pig-Aug*—pigeonite-augite), *Chr*—Cr-spinel, *Hbl*—hornblende, *Grt*—garnet, *Phl*—phlogopite, *Bt*—biotite, *Pl*—plagioclase, *Or*—orthoclase, *Qtz*—quartz, Ti-*Mag*—titanomagnetite, *Ilm*—ilmenite, *Ap*—apatite, *Zr*—zircon. Mineral end-members: *Wo*—wollastonite, *En*—enstatite, *Fs*—ferrosilite, *An*—anorthite.

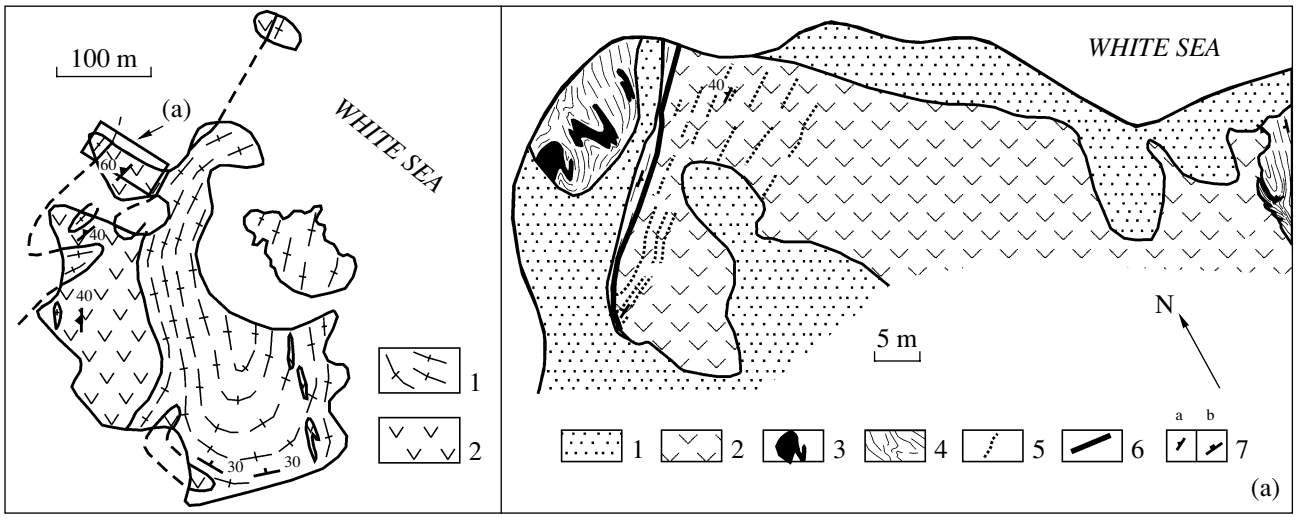

Fig. 7. Geological map of Gorelyi Island, Kandalaksha Archipelago, White Sea (prepared by E.V. Sharkov and A.V. Chistyakov). (1) Archean plagiomigmatites; (2) intrusion of plagioclase lherzolites–olivine gabbronorites. (a) Geological structure of the northern part of the intrusion. (1) Quaternary deposits; (2) olivine and olivine-free gabbronorites; (3) garnet amphibolite bodies; (4) gneisses and migmatites; (5) primary layering; (6) tectonic contact; (7) strikes and dips of: (a) gneissosity, (b) primary layering.

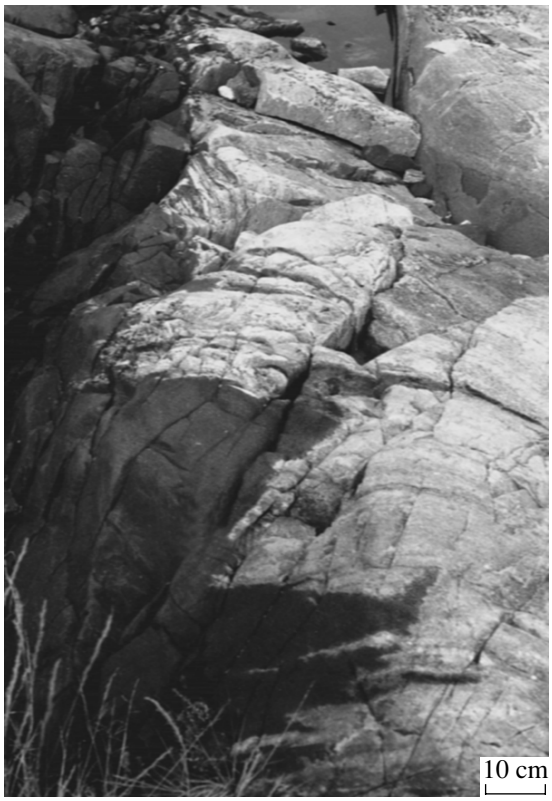

Fig. 8. Character of intrusive contacts of the Gorelyi island body (dark) with the host Archean plagiomigmatites (pale on the right-hand side of the photo). The photo clearly demonstrates that apophyses of fine-grained gabbroids penetrate into the host rocks. Photo: A.V. Chistyakov.

The *pyroxenites, melanocratic norites, and melanocratic gabbronorites* usually consist of orthopyroxene or, more rarely, orthopyroxene–clinopyroxene cumulates, sometimes with minor olivine amounts. The orthopyroxene is bronzite ($En_{76–78}$). The clinopyroxene commonly contains exsolution lamellae of broadly varying composition (Table 2). The intercumulus material usually contains alkaline feldspar, whose composition varies from K–Na varieties to nearly pure orthoclase. The *norites and gabbronorites* differ from them in containing cumulative *Pl*.

The *gabbronorites-anorthosites and anorthosites* are plagioclase cumulates, usually having coarse-grained textures. For example, anorthosites in the Northern Massif of Pezhostrov Island are dominated (75–95%) by subhedral cumulus plagioclase ($An_{65–73}$) slightly clouded by tiny inclusions of ore minerals. The intercumulus minerals include four distinct pyroxene types: (1) partly inverted *Pig* ($Wo_{14}En_{62}Fs_{24}$) with micrographic exsolution textures or inverted *Pig* with coarse clinopyroxene lamellae parallel to (001) in an orthopyroxene matrix, (2) inverted *Pig-Aug* with coarse orthopyroxene lamellae in clinopyroxene, (3) more rare *Opx* with thin *Cpx* lamellae parallel to (100), and (4) rare *Aug* with thin *Opx* lamellae. Both plagioclase and pyroxene usually show broad compositional variations even within a single hand-specimen. The compositional variability, the complete breakdown of the pigeonite solid solution, and the graphical exsolution textures of its breakdown suggest that the crystallization rate was high. Other intercumulus minerals are *Bt*, *Qtz*, *Or*, *Ilm*, Ti-*Mag*, *Ap*, and *Zr*.

The *magnetite gabbronorites and gabbro-diorites* were examined in the Cape Tolstik Massif, in which they occur together with gabbronorites and

Table 1. Representative analyses (wt %) of olivine

Component	18	704	705	V1	V7	P16	P30	P37
	OP	L	OGN	L	L	L	ON	L
SiO_2	37.63	37.90	37.51	36.67	37.07	37.87	38.08	37.61
FeO	24.29	22.55	24.03	18.74	25.29	20.25	20.70	21.95
MnO	0.17	0.34	0.21	0.23	0.21	0.27	0.25	0.28
MgO	38.41	38.83	37.5	42.3	36.93	42.68	41.06	39.45
NiO	0.43	0.28	0.58	0.65	0.59	0.38	0.50	0.57
Total	100.93	101.53	99.83	98.59	100.09	100.09	100.59	99.86
Si	0.98	0.99	0.99	0.95	0.98	0.96	0.98	0.98
Fe^{3+}	0.04	0.02	0.02	0.10	0.04	0.08	0.04	0.04
Fe^{2+}	0.49	0.47	0.51	0.31	0.52	0.34	0.40	0.44
Mn	0.00	0.01	0.00	0.01	0.00	0.01	0.01	0.01
Mg	1.49	1.51	1.48	1.64	1.46	1.61	1.57	1.53
Fo	0.74	0.75	0.74	0.80	0.72	0.79	0.78	0.76

Note: The crystal chemical formulas of minerals were calculated with a computer program developed by E.B. Kurdyukov and S.S. Abramov (IGEM RAS), *Fo* concentrations were calculated with the MINPET computer program. Sampling sites: 18—Anisimov Island; V1 and V7—Voronii Island; 704 and 705—Pezhostrov Island, Kandalaksha Bay, White Sea; P16—Shang Island; P30 and P37—Yudom-Navolok, Domashnyaya Bay, White Sea. Rocks (in this table and below): **L**—lherzolite, **OP**—olivine pyroxenite (*Ol* + *Opx* + *Cpx* cumulate), **PL**—plagioclase lherzolite (*Ol* + *Opx* + *Cpx* + *Pl*), **P**—pyroxenite (*Opx* + *Cpx*), **ON** and **OGN**—olivine norite and gabbronorite (*Opx* + *Cpx* + *Ol* + *Pl*), **GN**—gabbronorite (*Opx* + *Cpx* + *Pl*), **GA**—gabbronorite-anorthosite (*Pl*), **GD**—gabbrodiorite (*Pl* + *Cpx* + *Opx* + *Mag*), **MGN**—magnetite gabbronorite (*Pl* + *Cpx* + *Opx* + *Mag*).

anorthosites. These rocks are quite rich in titanomagnetites (up to 7–10 vol %). The relict minerals are inverted *Pig* or *Pig-Aug* and *Pl* ($An_{23–34}$).

The compositions of minerals and rocks in massifs of the complex and large layered plutons in the Baltic Shield are practically identical. The cumulus assemblages are always of two major types: (1) ultramafic cumulates (*Ol* ± *Chr*, *Ol* + *Opx* ± *Chr*, *Ol* + *Opx* + *Cpx* ± *Chr*, *Opx* ± *Cpx*, *Opx* + *Pl* ± *Ol*, and *Opx* + *Cpx* + *Pl* ± *Ol*), which are typical of the lower portions of the intrusions; and (2) mafic cumulates (*Opx* + *Pl* ± *Cpx*, *Pl*, and *Pig* + *Pig-Aug* + *Pl* ± *Mag*), which compose the upper parts of the intrusions. However, while all of these rocks in the plutons make up a single body, they occur in the complex as assemblages of small individual bodies with the corresponding compositions of their inner-contact zones, so that they can be collectively considered as if composing a large layered intrusion "separated" into fractions.

In contrast to the cumulates of the layered plutons, the rocks of the complex usually have elevated contents of intercumulus material (up to 25–35 vol %). In large layered intrusions, analogous contents of the intercumulus material are characteristic only of rocks in the marginal parts (Sharkov, 1980). Considered together with the aforementioned variability of the chemistry of minerals, their zonal character, and the often incomplete exsolution of the pigeonite pyroxene, these facts suggest that the coronite gabbro bodies were originally small in size and solidified in a regime typical of the marginal zones of large intrusions.

GEOCHEMISTRY

The contents of major, trace, and rare-earth elements in the rocks of the intrusions are presented in Tables 5–7. The whole rock series is classified as highly magnesian, with MgO contents attaining 27 wt %. Most of the rocks are low-Ti (TiO_2 < 1 wt %) and low- to

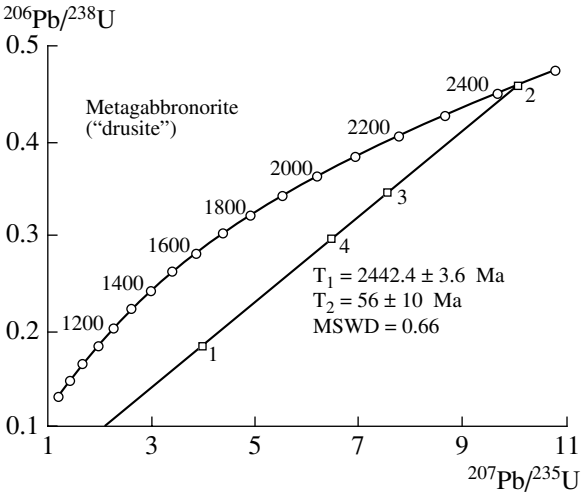

Fig. 9. U–Pb zircon isotopic dating of the olivine gabbronorite intrusion in Lodeinyi Island.

(1) Zircon from the host hornfels and migmatite at 0.5 m from the contact; (2) zircon from the central part of the "diffusion" contact zone; (3) zircon from the inner-contact gabbronorite at 0.5 m from the contact; (4) zircon from the olivine gabbronorites from the internal part of the body at 10 m from the contact.

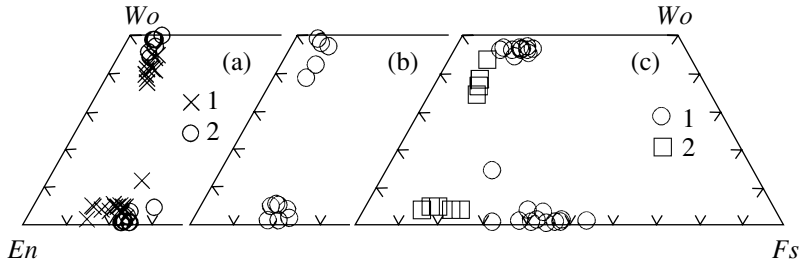

Fig. 10. Composition of pyroxenes in rocks of the drusite complex. (a) (1) Voronii Island, (2) Anisimov Island; (b) Yudom-Navolok and Shang Island intrusions; (c) Pezhostrov intrusion: (1) Southern Massif, (2) Northern Massif.

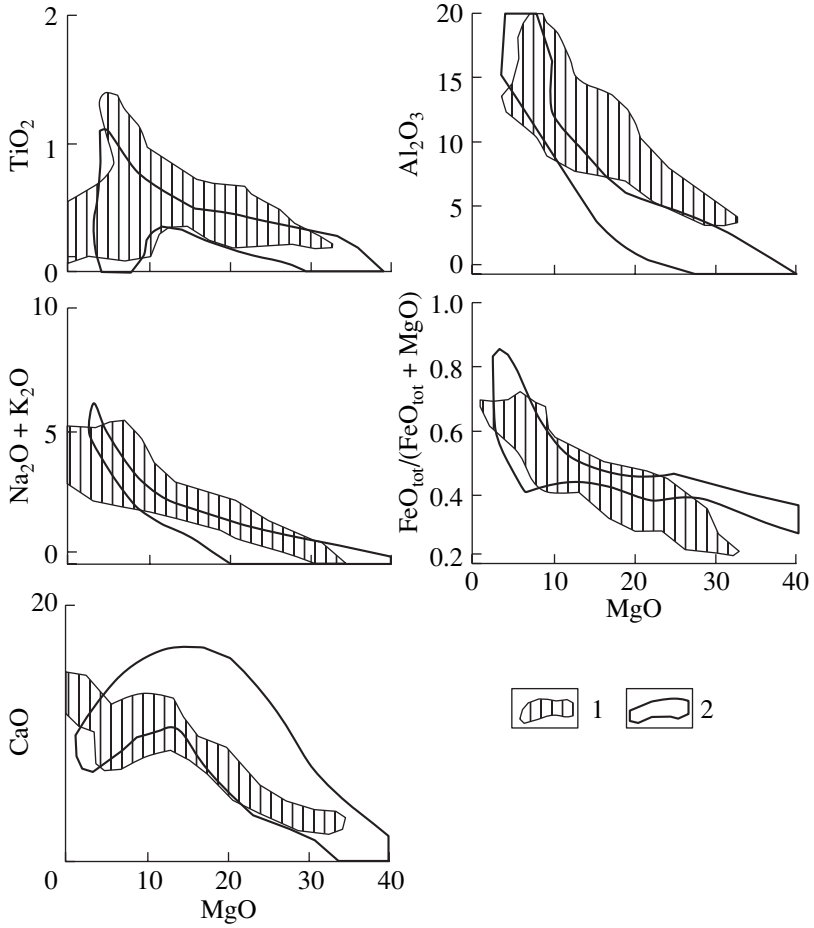

Fig. 11. Contents of major elements versus MgO in rocks of (1) the complex and (2) the Burakovsky layered intrusion. Here and below, comparative geochemical data on the Burakovsky pluton are given after (Chistyakov *et al.*, 2002).

moderate-Al, except only for the anorthosite and gabbronorite-anorthosite members of the complex, whose Al_2O_3 contents are as high as 20–27 wt %. The rocks exhibit relatively broad variations in the SiO_2 contents (up to 54 wt %), and some of them contain *Qtz* or are *Qtz*-normative.

Figure 11 demonstrates the contents of some major elements in the rocks in correlation with the MgO contents. The chemical variations within small and quite homogeneous bodies are insignificant, but the chemistry of the rocks notably varies from massif to massif. As can be seen from Fig. 11, rock compositions of the complex generally display the same relations as in the Burakovsky layered pluton in Karelia. Some differences exist only in the distribution of aluminum and calcium: the rocks containing from 10 to 30 wt % MgO include less aluminous and more calcic varieties, such as metasomatic clinopyroxenites, and this affects the configuration of the corresponding compositional fields.

It is worth noting that the REE patterns (Fig. 12) are absolutely analogous for all rock types within individ-

Table 2. Representative analyses (wt %) of pyroxenes

Component	18/1-1	18/1-2	18/7-1	18/7-2	704-1	705-1	705-2	705-3	707-1L	707-2L
	OP	OP	GN	GN	L	OGN	OGN	OGN	GN	GN
SiO_2	52.18	56.01	51.24	54.64	51.44	54.60	53.28	53.44	50.55	52.86
TiO_2	0.05	0.67	0.00	0.22	0.17	0.07	0.08	0.36	0.01	
Al_2O_3	0.85	0.85	0.62	3.04	3.23	1.34	2.59	2.50	0.90	1.05
Cr_2O_3	0.00	0.60	0.00	0.20	1.43	0.53	0.90	0.39	0.00	0.00
FeO	16.99	4.82	16.44	4.49	7.13	13.37	6.72	5.71	29.26	8.79
MnO	0.39	0.15	0.18	0.05	0.20	0.17	0.11	0.14	0.44	
MgO	29.32	16.27	29.70	13.73	19.03	27.42	18.23	15.84	18.00	13.94
CaO	0.22	20.86	0.43	22.51	16.70	2.01	17.72	20.42	0.33	22.33
Na_2O		0.27		1.23	0.51	0.12	0.37	0.95	0.42	0.57
Total	100.00	100.50	98.61	100.11	99.84	99.63	100.00	99.75	99.91	99.54
Si	1.87	2.05	1.85	2.00	1.87	1.96	1.94	1.96	1.94	1.97
Ti	0.00	0.02	0.00	0.01	0.00	0.00	0.00	0.01	0.00	0.00
Al	0.04	0.04	0.03	0.13	0.14	0.06	0.11	0.11	0.04	0.05
Cr	0.00	0.02	0.00	0.01	0.04	0.02	0.03	0.01	0.00	0.00
Fe^{3+}	0.22	0.00	0.27	0.00	0.10	0.00	0.00	0.01	0.12	0.05
Fe^{2+}	0.29	0.15	0.23	0.14	0.12	0.40	0.20	0.16	0.82	0.22
Mn	0.01	0.00	0.01	0.00	0.01	0.01	0.00	0.00	0.01	0.00
Mg	1.56	0.89	1.60	0.75	1.03	1.47	0.99	0.86	1.03	0.77
Ca	0.01	0.82	0.02	0.88	0.65	0.08	0.69	0.80	0.01	0.89
Na	0.00	0.02	0.00	0.09	0.04	0.01	0.03	0.07	0.03	0.04
Wo	0.4	44.0	0.8	49.8	34.2	4.0	36.6	43.4	0.7	46.0
En	74.7	47.8	75.5	42.3	54.1	75.2	52.4	46.9	51.6	39.9
Fs	24.9	8.2	23.7	7.8	11.7	20.8	11.0	9.7	47.7	14.1
Component	707-1m	707-2m	Pzh8-L	Pzh8-m	V7-1	V7-2	V8-1	V8-2	Lod-1	P16-1cor
	GN	GN	GN	GN	L	L	P	P	GN	L
SiO_2	52.36	51.66	53.45	52.87	53.55	54.36	52.78	52.48	53.15	53.86
TiO_2	0.16	0.05	0.15	0.00	0.18	0.33	0.12	0.33	0.12	0.00
Al_2O_3	1.32	0.42	1.32	0.70	3.04	2.89	2.63	2.91	1.79	0.85
Cr_2O_3	0.00	0.00	0.16	0.04	1.07	0.16	1.37	0.34	0.00	0.00
FeO	10.16	25.94	9.32	25.71	5.98	4.67	13.65	5.61	17.83	12.14
MnO	0.33	0.24	0.14	0.37	0.13	0.08	0.27	0.12	0.20	0.27
MgO	12.32	20.83	13.86	19.70	17.00	15.09	23.02	15.41	26.14	31.18
CaO	22.52	0.32	21.14	0.63	17.85	20.34	5.65	20.96	0.62	0.29
Na_2O	0.66	0.22	0.59	0.00	0.98	0.92	0.19	1.08	0.14	0.00
Total	99.83	99.68	100.13	100.02	99.78	98.84	99.68	99.24	99.99	98.59
Si	1.97	1.95	1.99	2.00	1.96	2.01	1.93	1.93	1.93	1.92
Ti	0.00	0.00	0.00	0.00	0.00	0.01	0.00	0.01	0.00	0.00
Al	0.06	0.02	0.06	0.03	0.13	0.13	0.11	0.13	0.08	0.04
Cr	0.00	0.00	0.00	0.00	0.03	0.00	0.04	0.01	0.00	0.00
Fe^{3+}	0.05	0.09	0.00	0.00	0.00	0.00	0.00	0.06	0.07	0.12
Fe^{2+}	0.27	0.73	0.29	0.81	0.18	0.14	0.42	0.11	0.47	0.25
Mn	0.01	0.01	0.00	0.01	0.00	0.00	0.01	0.00	0.01	0.01
Mg	0.69	1.17	0.77	1.11	0.92	0.83	1.25	0.84	1.41	1.66
Ca	0.91	0.01	0.84	0.03	0.70	0.81	0.22	0.83	0.02	0.01
Na	0.05	0.02	0.04	0.00	0.07	0.07	0.01	0.08	0.01	0.00
Wo	47.1	0.6	44.2	1.3	38.6	45.2	11.6	44.7	1.2	0.5
En	35.8	58.3	40.3	56.6	51.1	46.6	66.0	45.7	71.2	81.3
Fs	17.1	41.1	15.4	42.1	10.3	8.2	22.4	9.5	27.6	18.2

Table 2. (Contd.)

Component	P16-2	P30-c	P30r	P37-1	P37-1cor	P37-2cor	t1-1	t1-2	t2-1L	t2-1m
	L	ON	ON	PL	PL	PL	GD	GD	GD	GD
SiO_2	50.68	52.87	52.09	53.50	52.84	52.69	53.54	52.39	49.02	51.94
TiO_2	0.32	0.08	0.50	0.10	0.22	0.00	0.00	1.31	0.00	0.24
Al_2O_3	4.48	1.36	1.79	1.27	3.21	1.76	1.50	2.13	0.70	2.03
Cr_2O_3	1.04	0.45	0.19	0.42	0.91					
FeO	5.26	12.38	13.93	11.36	4.22	13.53	16.11	4.74	35.49	13.20
MnO	0.12	0.21	0.25	0.22	0.12	0.25	0.27	0.09	0.59	0.06
MgO	13.98	29.29	28.62	30.28	15.19	29.77	25.80	15.22	13.65	10.21
CaO	20.89	2.49	1.89	2.38	22.43	0.32	2.58	23.60	0.39	21.32
Na_2O	1.46			0.28	1.16			0.49	0.11	0.94
Total	98.23	99.13	99.26	99.81	100.30	98.32	99.80	99.97	99.95	99.94
Si	1.89	1.89	1.87	1.89	1.92	1.90	1.94	1.93	1.94	1.97
Ti	0.01	0.00	0.01	0.00	0.01	0.00	0.00	0.04	0.00	0.01
Al	0.20	0.06	0.08	0.05	0.14	0.07	0.06	0.09	0.03	0.09
Cr	0.03	0.01	0.01	0.01	0.03	0.00	0.00	0.00	0.00	0.00
Fe^{3+}	0.09	0.14	0.14	0.17	0.06	0.13	0.05	0.02	0.09	0.02
Fe^{2+}	0.07	0.23	0.27	0.16	0.06	0.28	0.44	0.13	1.08	0.39
Mn	0.00	0.01	0.01	0.01	0.00	0.01	0.01	0.00	0.02	0.00
Mg	0.77	1.56	1.53	1.59	0.82	1.60	1.40	0.83	0.81	0.58
Ca	0.83	0.10	0.07	0.09	0.87	0.01	0.10	0.93	0.02	0.87
Na	0.11	0.00	0.00	0.02	0.08	0.00	0.00	0.03	0.01	0.07
Wo	46.9	4.7	4.4	47.8	0.6	5.0	48.6	0.8	46.5	4.4
En	43.7	77.0	78.7	45.0	78.9	70.0	43.6	39.9	31.0	78.7
Fs	9.4	18.3	16.9	7.2	20.5	24.9	7.8	59.2	22.6	16.9

Note: Kandalaksha Bay, White Sea: samples 18/1 and 18/7—Anisimov Island; V7 and V8—Voronii Island; Lod1—Lodeinyi Island; 704, 705, 707, and Pzh8—Pezhostrov Island; t1, t2—Cape Tolstik (T.L. Larikova's data). Domashnyaya Bay, White Sea: P16—Shang Island; P30 and P37—Yudom-Navolok. Sample numbers are supplemented with the following indices denoting the grain or grain part analyzed: *c*—grain core, *r*—grain rim; in the presence of exsolution textures, *L*—lamella (lamellae), *m*—matrix, *cor*—drusite corona. The crystal chemical formulas of minerals were calculated with the Make-Mineral-19 computer program (E.B. Kurdyukov and S.S. Abramov, IGEM RAS), *Wo*, *En*, and *Fs* contents were calculated with the MINPET computer program. Here and below, the absence of data means contents below the analytical detection limit.

Table 3. Representative analyses (wt %) of Cr-spinel

Component	V1-1	V1-2	V8	704	705-1	705-2	P16-1
	L	L	P	L	OGN	OGN	L
TiO_2	0.93	2.99	0.40	0.03	0.42	0.70	
Al_2O_3	19.12	14.57	15.55	15.72	20.61	16.78	43.25
FeO	43.59	45.32	28.24	29.8	33.2	33.6	24.96
MnO	0.09	0.10	0.04	0.40	0.35	0.39	
Cr_2O_3	33.73	35.27	49.52	46.86	40.10	43.55	22.77
MgO	2.53	2.22	5.07	5.66	3.79	3.97	9.14
NiO	0.20	0.27	0.08	0.24	0.55	0.06	0.17
V_2O_3	0.84	0.57	0.41	0.45	0.32	0.32	
ZnO	0.06	0.06	0.42				0.20
Total	101.09	101.37	99.73	99.16	99.34	99.37	100.49
Al	0.74	0.58	0.62	0.62	0.81	0.67	1.47
Cr	0.88	0.94	1.31	1.24	1.05	1.16	0.52
Fe^{3+}	0.34	0.33	0.05	0.14	0.12	0.14	0.01

Note: Cr-spinel compositions are normalized to 4 oxygen atoms. See Table 1 for sampling sites and rock names.

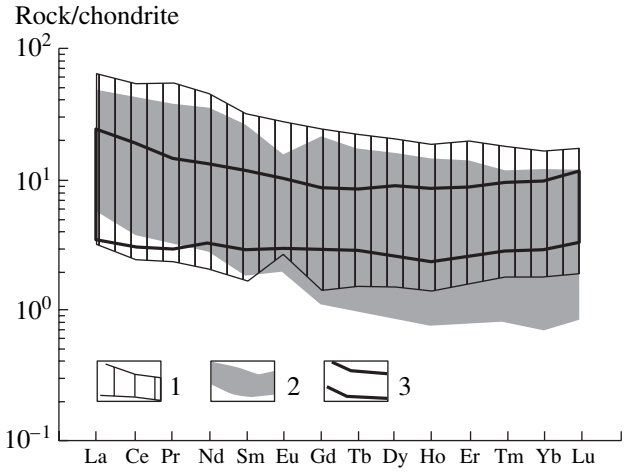

Fig. 12. Chondrite-normalized REE patterns of the rocks. (1) Coronite complex; (2) Burakovsky pluton; (3) boninites from the Izu-Bonin island arc (Murton *et al.*, 1992).

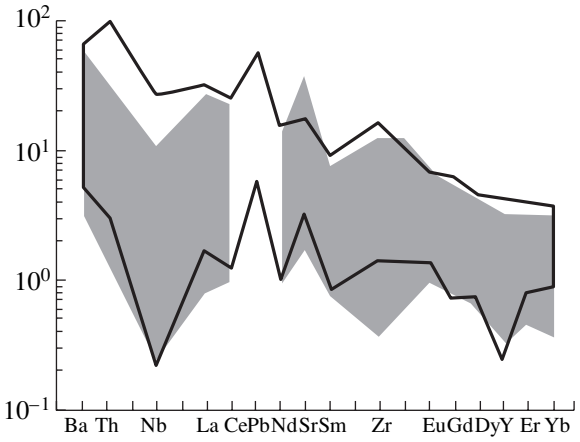

Fig. 13. Spidergram of primitive mantle-normalized contents of trace elements in rocks of the drusite complex and the Burakovsky pluton (dark).

ual bodies and for all massifs as a whole, which testifies for the homogeneity of the parental magmas of all intrusions in the complex. The Eu anomalies are insignificant (if any) and are controlled by the plagioclase concentrations in the rocks. The rocks of the complex are typically enriched in LREE, with the Ce/Yb ratio as high as 5.65, and flat patterns for HREE. The REE patterns of the rocks practically completely overlap with the fields for rocks composing the layered series of the Burakovsky pluton. Both fields completely overlap the field of boninites from the modern Izu–Bonin island arc, a fact providing evidence of genetic similarities between these rocks.

The spidergrams with trace-element contents normalized to the primitive mantle (Fig. 13) provide additional geochemical criteria pointing to genetic links between the rocks of this complex and the Burakovsky layered pluton. These links are manifested in the similar character of distribution of trace elements in the rocks, which are enriched in incompatible elements (Ba, Zr, Th, La, and others) and depleted in HFSE (Nb, Y, and others).

Available data indicate that the εNd (2.45) value for the rocks of the complex ranges from +0.2 to –1.8 (Lobach-Zhuchenko *et al.*, 1998), which is characteristic of the rocks of large layered intrusions in the neighboring cratons (Amelin *et al.*, 1995; Sharkov *et al.*, 1997) and of the coeval basalts in the riftogenic Vetreny Belt in the Karelian craton (Puchtel *et al.*, 1997).

Thus, the rock assemblage of the mafic–ultramafic complex in the BMB and layered plutons in the nearby cratons show almost invariable and identical compositional characteristics. These are their similar rock assemblages, from ultramafic to leucocratic cumulates and magnetite gabbrodiorites with similar compositions of their minerals. Geochemical data also point to these similarities: analogously to the rocks of the layered intrusions, the rocks of the complex are low in Ti and Nb and high in LREE at small negative εNd (2.45) values. All of these features led us to attribute the rocks of the complex to the crystallization products of a silicic high-Mg (boninite-like) series (SHMS).

DISCUSSION

General geological characteristics of the drusite complex. As was mentioned above, the intrusions of this complex in Belomorie are a component of the large Early Paleoproterozoic Baltic SHMS igneous province. However, manifestations of coeval magmatism of similar character were basically different in the cratons and mobile belts (BMB and TLMB) between them. While this magmatism produced large layered intrusions, dike swarms, and volcanic sheets in the cratons, in the mobile belts it was characterized, first and foremost, by dispersed magmatic activity, which did not give rise to dike swarms. Volcanic sheets comagmatic with the intrusions of the complex are widespread along the northeastern boundary of the BMB, near its boundaries with the Main Lapland Thrust. These metavolcanics, which were produced by SHMS melts and have ages of 2.45–2.40 Ga, can be traced throughout the whole northeastern shore of Kandalaksha Bay up to Por'ya Bay, where they are components of the Kandalaksha Formation (Priyatkina and Sharkov, 1979). These rocks are known in Finland as the Tana Complex (Barbey and Raith, 1990; Belyaev and Kozlov, 1997; Sharkov and Smolkin, 1997). Intense Svecofennian (Karelian) metamorphism transformed them mostly in garnet amphibolites, which locally exhibit relict volcanic textures (Priyatkina and Sharkov, 1979). Tectonic blocks of these amphibolites also occur among migmatites in some islands of the Kandalaksha Archipelago, for example, in Voronii Island (authors' data). All of these

Table 4. Composition (wt %) of biotite

Component	P16	P30	P37	705	707	V1	V7	V8
	L	ON	L	OGN	GN	L	L	P
SiO_2	38.68	38.32	38.85	38.99	38.94	38.94	40.52	39.58
TiO_2	4.27	7.62	6.64	7.05	5.41	7.19	5.79	5.49
Al_2O_3	16.04	15.08	15.74	14.06	14.90	16.48	15.42	14.91
Cr_2O_3	0.63	0.48	0.34	0.11	n.a.	0.20	0.25	0.29
FeO	6.20	8.75	8.32	14.56	14.94	9.56	7.26	6.90
MnO					0.04			
MgO	19.29	16.70	16.5	14.66	15.49	16.33	19.45	19.04
CaO			0.11					
K_2O	9.48	9.29	9.60	10.00	9.85	9.54	9.56	9.71
Na_2O	0.44	0.35	0.15	0.35	0.42	0.24	0.42	0.19
NiO	0.22	0.25	0.43	n.a.	n.a.	0.18	0.18	0.22
Total	95.25	96.84	96.68	99.78	99.99	98.66	98.85	96.33
Si	2.87	2.88	2.92	2.88	2.84	2.87	2.92	2.93
Ti	0.24	0.43	0.37	0.39	0.30	0.40	0.31	0.31
Al	1.40	1.33	1.39	1.22	1.28	1.43	1.31	1.30
Al^{IV}	1.13	1.12	1.08	1.12	1.16	1.13	1.08	1.07
Al^{VI}	0.28	0.21	0.31	0.10	0.13	0.30	0.23	0.23
Fe^{3+}	0.00	0.00	0.00	0.00	0.00	0.00	0.00	0.00
Fe^{2+}	0.38	0.55	0.52	0.90	0.91	0.59	0.44	0.43
Mn	0.00	0.00	0.00	0.00	0.00	0.00	0.00	0.00
Mg	2.14	1.87	1.85	1.61	1.69	1.79	2.09	2.10
Ca	0.00	0.00	0.01	0.00	0.00	0.00	0.00	0.00
Na	0.06	0.05	0.02	0.05	0.06	0.03	0.06	0.03
K	0.90	0.89	0.92	0.94	0.92	0.90	0.88	0.92
Mg/Fe	2.41	1.48	1.54	0.50	0.74	1.33	2.08	2.14

Note: The crystal chemical formulas of minerals were calculated with the Make-Mineral-19 computer program (E.B. Kurdyukov and S.S. Abramov, IGEM RAS). See Table 1 for sampling sites and rock names; n.a.—not analyzed.

facts suggest that the emplacement of these intrusions was associated with lava flows on the surface.

Conditions under which the intrusions of the complex were produced. Unlike other magmatic complexes of the large Baltic SHMS province, some features of the complex characterize its rocks as the crystallization products in a mobile environment. These features are as follows: (1) the small sizes of the bodies and their wide lateral distribution; (2) the petrography of the rocks, suggesting their rapid solidification; (3) the morphology of the bodies, which often implies that these bodies filled detachment voids in folds; (4) numerous distortions of the primary magmatic layering; (5) the bodies themselves and their host rocks are often cut by basite dikes along shear zones, with these dikes also produced by the SHMS melts; (6) the mafic–ultramafic bodies of the complex originally had different orientation and were then variably reworked, which suggests that there are more than one generations of intrusion of different ages (in this situation, the aforementioned dikes could have served as feeders for younger intrusions); and (7) the spatial distribution of the intrusions is controlled by different Early Paleoproterozoic stress field orientations in the BMB.

The character of the contacts of the intrusions. The host rocks of these intrusions most often belong to the Archean complex of gray gneisses. More rarely, these intrusions cut aluminous garnet–biotite gneisses, whose protoliths were supracrustal rocks.

Primary intrusive contacts of the bodies with their host rocks and xenoliths of the latter in the basites were found at all of the intrusive bodies. It was difficult to identify hot contact hornfels and details of the reaction interactions during the emplacement because both the wall rocks and the basites themselves were significantly recrystallized during the Karelian (Svecofennian) meta-

Table 5. Composition (wt %) of rocks from massifs of the drusite complex

Component	104*	V7	V8	V12	V16	G2	L4	Lod2	P3	P8	P24/1	P29
	1	2	3	4	5	6	7	8	9	10	11	12
	GN**	L	P	OGN	GN	P	GN	N	OGN	L	L	PL
SiO_2	48.75	48.85	50.50	46.50	51.30	53.25	53.80	56.60	49.10	47.70	48.65	50.90
TiO_2	1.10	0.68	0.53	0.34	0.24	0.83	0.80	0.65	0.50	0.30	0.24	0.53
Al_2O_3	17.95	7.40	10.50	17.30	17.70	7.40	12.70	13.40	9.35	6.00	7.00	8.60
Fe_2O_3	0.37	1.13	0.89	0.13	1.21	0.75	0.93	1.43	0.86	4.38	0.45	1.27
FeO	10.09	10.77	9.82	11.04	6.91	8.73	9.24	6.23	10.65	8.93	9.50	9.25
MnO	0.16	0.19	0.17	0.14	0.16	0.18	0.16	0.08	0.19	0.18	0.14	0.17
MgO	7.92	20.99	16.76	12.13	9.09	13.19	9.11	6.61	18.18	25.00	25.96	20.24
CaO	10.11	7.36	8.68	9.23	9.78	12.49	8.66	7.59	6.87	5.00	4.89	6.21
Na_2O	1.80	1.05	1.35	2.19	2.39	1.97	2.54	3.71	1.60	0.83	1.05	1.39
K_2O	0.36	0.34	0.33	0.35	0.19	0.52	1.28	1.89	0.65	0.23	0.29	0.65
P_2O5	0.12	0.08	0.08	0.07	0.03	0.09	0.13	0.13	0.10	0.06	0.11	0.10
Total	98.73	98.84	99.61	99.42	99.00	99.40	99.35	98.32	98.05	98.61	98.28	99.31
Component	P42	P82/7	P99	P101	P102	P107/2	P108/7	Pzh13	704	705	708	742/25
	13	14	15	16	17	18	19	20	21	22	23	24
	OGN	GN	P	L	GN	PL	OGN	MGN	L	OGN	GA	GD
SiO_2	52.60	52.65	54.00	49.50	53.80	50.35	51.00	50.46	49.67	51.42	52.09	51.89
TiO_2	0.24	0.38	0.24	0.20	0.68	0.47	0.58	2.57	0.31	0.43	0.40	1.82
Al_2O_3	11.80	16.60	4.70	8.00	16.90	8.50	10.50	12.84	7.78	11.29	22.07	13.12
Fe_2O_3	0.10	1.30	0.65	1.85	0.52	1.28	1.68	1.27	2.65	1.48	1.40	3.86
FeO	8.45	5.22	7.96	9.90	6.82	9.51	9.29	13.40	8.98	7.98	5.13	11.58
MnO	0.15	0.12	0.18	0.20	0.13	0.18	0.17	0.21	0.15	0.14	0.08	0.15
MgO	16.92	8.48	26.08	21.91	7.82	19.93	16.69	4.92	23.76	16.23	4.54	4.47
CaO	7.53	10.60	4.01	6.01	8.02	6.73	6.76	9.34	4.36	7.11	9.14	8.52
Na_2O	1.55	3.31	0.83	1.02	3.13	1.52	1.90	2.45	0.85	2.11	3.53	2.91
K_2O	0.42	0.61	0.21	0.17	1.07	0.60	0.78	0.39	0.36	0.47	0.59	0.79
P_2O5	0.05	0.07	0.04	0.02	0.11	0.08	0.09	0.00	0.09	0.13	0.09	0.12
Total	99.81	99.34	98.90	98.78	99.00	99.15	99.44	98.85	98.96	98.79	99.06	99.35

Note: The sampling sites were at Kandalaksha Bay (1–8, 20–24) and Domashnyaya Bay (9–19) of the White Sea: Anisimov Island—1, Voronii Island—2–5, Gorelyi Island—6, Lodeinyi Island—7–8, Shang Island—9–10, Yudom-Navolok—11–19, Pezhostrov Island—20–23, Cape Tolstik—24 (Bogdanova, 1996). * Sample numbers; ** cumulate.

morphic event at $T = 650$–700°C and $P = 9$–10 kbar (Larikova, 2000). Neither the wall rocks nor the xenoliths exhibit any traces of hot hornfels, because the inner-contact gabbro is transformed into amphibolite with an apogabbro texture, and the outer-contact rocks and xenoliths gave rise (depending on their composition) to nematogranoblastic amphibolites or biotite or biotite–garnet gneisses with green hornblende and low-Ti biotite. Also, it seems to be impossible to determine the grade of the regional Late Archean metamorphism of the host rocks before the emplacement of the basites, because the local Karelian assemblages are of prograde character and contain progradely zoned garnet grains. It is worth noting that the mineral assemblages of the host rocks and apogabbro coronites were metamorphosed under identical *P–T* conditions and define a single evolutionary *P–T* path, which is possible only if the Late Archean metamorphism of the host rocks occurred at lower *P–T* parameters than the Karelian metamorphism, although this metamorphism occurred elsewhere in Belomorie under higher pressures or higher temperatures.

The tectonic contacts of the intrusive bodies are often marked with zones of Karelian migmatization,

Table 6. Trace-element contents (ppm) in representative rock samples

Element	V8	V12	V14	V16	G2	L4	Lod2	P3	P8	P241	P29	P42	P97	P99	P101	P107/2	P108/7
	P	OGN	GN	GN	P	GN	GN	OGN	L	L	PL	OGN	GN	P	L	PL	OGN
V	217	88	135	110	213	208	171	204	175	137	160	159	179	142	133	40	161
Co	69	58	38	53	53	45	44	78	97	79	62	66	35	77	84	13	74
Ni	394	341	121	146	279	118	74	506	867	948	682	430	94	585	757	14	526
Cu	94	95	49	66	67	98	45	123	49	77	71	51	59	39	33	39	33
Zn	92	85	55	75	70	77	104	108	109	92	78	82	62	81	95	49	74
Rb	14	20	12	7	22	18	42	24	10	17	17	16	10	14	10	228	26
Sr	99	134	213	226	178	241	236	127	81	71	150	215	314	54	141	67	179
Y	3	0	1	1	7	13	15	4	3	5	6	2	16	3	3	49	4
Zr	45	62	38	0	84	110	154	58	16	57	77	32	121	48	28	461	68
Nb	4	1	0	8	3	4	9	6	5	1	2	6	3	4	3	15	5
Ba	149	129	87	97	215	400	395	258	125	147	249	185	368	123	110	705	293
Pb	2	7	1	5	0	7	10	2	1	0	2	5	6	1	3	148	5
Th	1	4	3	1	2	7	4	5	4	2	8	3	1	2	2	1	1
Sc	32	19	31	28	32	22	26	26	21	15	20	19	25	15	19	0	17

Note: See Table 5 for sampling sites (others: sample P97—Yudom-Navolok, sample V14–Voronii Island).

often with breccias, in which angular fragments of gabbroid bodies are transformed into amphibolites and cemented by granitic material. In contrast to the ancient plagiomigmatites, this material usually consists of pink potassic granitoids. Weakly altered magmatic rocks with primary magmatic textures and structures are usually preserved only in the central portions of the bodies.

The age of the mafic–ultramafic complex. The age of the magmatic crystallization of the intrusive bodies varies from 2.46 to 2.36 Ga (Aleksejev *et al.*, 2000; Bibikova *et al.*, 1993; Kaulina and Kudryashov, 2000; Slabunov *et al.*, 2001; Balaganskii *et al.*, 1997). These age values coincide with the ages of large layered intrusions in the nearby Karelian craton (Amelin *et al.*, 1995; Chistyakov *et al.*, 2002). Many of the bodies are often intersected by pink potassic granites with an age of 2.41 Ga (Bibikova *et al.*, 1993; Zindler *et al.*, 1996).

As is evident from the facts presented above, SHMS magmatism in the BMB and the neighboring Karelian craton continued over a significant age interval in the Early Paleoproterozoic, at least from 2.46 Ga (Pezhostrov Massif) until 2.36 Ga (Zhemchuzhnyi Massif in the Kola Peninsula), i.e., approximately 100 m.y. As is evident from the above materials, there seems to be no correlations between the ages of the intrusions and their compositions.

The feeders of the new intrusions are partly preserved in the form of dikes cutting across already-solid intrusions of the complex, which were still not deformed (as in Anisimov Island) or were deformed along blastomylonitization zones, as can be clearly seen in the Pezhostrov Island and Cape Tolstik intrusions. Fragments of analogous dikes were also found in the host rocks in the form of boudinaged amphibolite bodies. The magmatic activity seems to have continued and has not been interrupted by the reorientation of the stress field in the upper crust. This ensured the wide spread of the small intrusions within the BMB.

The main episode of the tectono-metamorphic reworking of the BMB took place at about 1.9–1.8 Ga (Bogdanova, 1996; Zinger *et al.*, 1996; Aleksejev *et al.*, 1999; Kaulina and Kudryashov, 2000; Larikova, 2000; Bibikova *et al.*, 2004) and was related to the development of the Svecofennian (Late Paleoproterozoic) Main Lapland Thrust (Priyatkina and Sharkov, 1979). The corona textures and amphibolization of the mafic rocks seem to have developed during exactly this time period. This is consistent with the age values obtained for metamorphic apatite, garnet, and rutile from the anorthosites exposed in Pezhostrov and Voronii islands (see above). Also, then most basite bodies in the Kandalaksha part closest to the fault were boudinaged and acquired a secondary northwestern orientation.

Distinctive structural features of the BMB magmatic systems. The obvious similarities between the rocks composing the complex and layered intrusions in the cratons suggest that all of these rocks were produced by similar SHMS melts. According to geochemical and isotopic–geochemical data, these melts were generated by the large-scale assimilation of Archean crustal rocks by ultramafic mantle melts (Amelin and Semenov, 1996; Puchtel *et al.*, 1997; Sharkov *et al.*, 1997). The most probable mechanism that generated these melts was the ascent of magma chambers through the crust according to the zone-refinement mechanism (Sharkov *et al.*, 1997), i.e., by means of the simultaneous melting

Table 7. REE contents (ppm) in the rocks

Component	V1	V7	V8	V12	V14	V16	L4	Lod3/2	AN	G2	P3
	L	L	P	OGN	GN	GN	GN	GN	GN	P	OGN
La	3.1	4.1	3.9	3.5	1.8	1.0	11.7	7.2	3.6	10.4	6.7
Ce	6.9	9.1	8.6	7.5	3.9	2.0	24.5	15.2	8.0	23.9	14.4
Pr	0.90	1.19	1.14	0.94	0.53	0.29	3.00	1.90	1.07	3.25	1.81
Nd	3.80	5.10	5.00	4.07	2.50	1.20	11.90	7.53	4.51	13.60	7.40
Sm	0.98	1.26	1.17	0.96	0.56	0.32	2.49	1.52	1.15	3.25	1.67
Eu	0.31	0.37	0.39	0.42	0.28	0.20	0.63	0.58	0.41	0.88	0.47
Gd	1.12	1.37	1.34	1.04	0.70	0.36	2.25	1.40	1.30	2.70	1.71
Tb	0.18	0.22	0.22	0.17	0.13	0.07	0.33	0.22	0.21	0.39	0.27
Dy	1.16	1.47	1.43	1.15	0.82	0.48	2.08	1.38	1.37	2.25	1.70
Ho	0.24	0.32	0.31	0.24	0.18	0.10	0.44	0.28	0.29	0.44	0.36
Er	0.73	0.91	0.89	0.72	0.57	0.33	1.23	0.78	0.82	1.17	1.01
Tm	0.10	0.13	0.13	0.10	0.09	0.06	0.18	0.11	0.12	0.14	0.15
Yb	0.71	0.88	0.85	0.68	0.64	0.37	1.12	0.75	0.78	0.95	1.02
Lu	0.11	0.14	0.14	0.09	0.10	0.06	0.17	0.12	0.12	0.13	0.16
Total	20.34	26.56	25.51	21.58	12.8	6.84	62.02	38.97	23.75	63.45	38.83
$(La/Nd)_n$	1.56	1.54	1.49	1.65	1.38	1.60	1.88	1.83	1.53	1.46	1.73
$(Ce/Yb)_n$	2.47	2.63	2.57	2.81	1.55	1.37	5.56	5.15	2.61	6.40	3.59
Component	P8	P16	P24/1	P29	P35/9	P37	P42	P97	P99	P101	P108/7
	L	L	L	PL	OGN	L	OGN	GN	P	L	OGN
La	2.3	2.9	4.9	6.9	3.3	2.8	4.8	14.7	3.3	2.4	9.9
Ce	5.4	6.2	9.8	14.7	6.6	6.0	10.0	31.4	6.9	5.4	20.8
Pr	0.72	0.81	1.31	1.83	0.86	0.78	1.26	3.94	0.89	0.75	2.55
Nd	3.10	3.40	5.28	7.30	3.64	3.20	5.15	15.10	3.65	3.44	10.10
Sm	0.71	0.81	1.12	1.49	0.81	0.75	1.04	3.45	0.79	0.88	2.16
Eu	0.23	0.25	0.23	0.40	0.22	0.24	0.37	0.98	0.25	0.29	0.62
Gd	0.76	0.80	1.03	1.48	0.79	0.80	1.00	3.19	0.75	1.02	2.17
Tb	0.12	0.13	0.16	0.22	0.14	0.13	0.15	0.48	0.12	0.16	0.32
Dy	0.80	0.86	1.06	1.37	0.81	0.76	0.99	2.91	0.80	0.98	2.08
Ho	0.17	0.18	0.21	0.27	0.16	0.17	0.19	0.60	0.16	0.21	0.42
Er	0.51	0.52	0.68	0.79	0.47	0.48	0.55	1.59	0.55	0.59	1.18
Tm	0.07	0.07	0.09	0.11	0.07	0.06	0.08	0.24	0.08	0.08	0.17
Yb	0.51	0.48	0.64	0.74	0.49	0.45	0.45	1.52	0.48	0.59	1.13
Lu	0.08	0.07	0.09	0.11	0.06	0.07	0.08	0.23	0.08	0.09	0.17
Total	15.48	17.48	26.60	37.71	18.42	16.69	26.11	80.33	18.76	16.83	53.74
$(La/Nd)_n$	1.42	1.63	1.78	1.81	1.74	1.68	1.79	1.86	1.73	1.32	1.87
$(Ce/Yb)_n$	2.69	3.29	3.89	5.05	3.43	3.39	5.65	5.25	3.63	2.32	4.68

Note: Ratios are normalized to chondrite. See Table 5 for sampling sites (others: samples V1 and V14—Voronii-Island, AN—Anisimov Island, Lod3/2—Lodeinyi Island, P16—Shang Island, P35/9, P37, and P97—Yudom-Navolok).

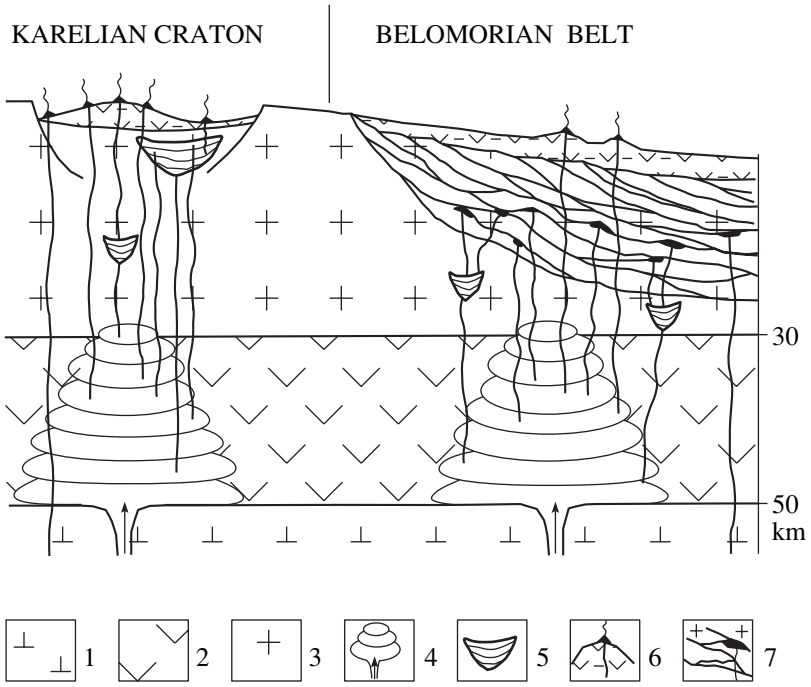

Fig. 14. Model for the structure of magmatic systems beneath cratons and intercratonic mobile belts of the Baltic Shield.
(1) Ancient lithospheric mantle; (2) Archean basite lower crust; (3) Archean sialic crust; (4) region where the magma chambers ascends according to the floating-zone mechanism; (5) layered intrusions; (6) sedimentary–volcanic rocks and lava plateaus; (7) zone of tectonic flowage of the Belomorian belt with small mafic–ultramafic bodies (black).

of the roof rocks and crystallization of the melt near the bottom (Fig. 14).

The differences in the character of intrusive magmatism were obviously related to the mobility of the environments through which the melts passed *en route* from the magma-generating regions to the surface. In the rigid crust of the cratons, the melts ascending from the evolving deep-seated chambers accumulated in the same intrusive chambers, which progressively expanded with their replenishment with newly arrived magma portions. This process resulted in the origin of large intrusive bodies, which included the crystallization products of all of these melts and the whole set of the corresponding cumulates. In places, complexes were formed consisting of two or more large intrusions, such as the Burakovsky and Monchegorsk complexes (Chistyakov *et al.*, 2002; Sharkov *et al.*, 2002). Judging by isotopic–geochemical data, they were long-lived magmatic centers, whose lifetime was at least 50 m.y.

The same rocks occur in the BMB as small individual intrusions. Evidently, because the material of the belt remained mobile for a long time, melt portions newly arriving from beneath could be accommodated only in small chambers, which were controlled by local structural heterogeneities (folds, detachments, local extension zones, etc.) that were continuously generated in the process of the tectonic flowage of the country rocks. Furthermore, these chambers were constantly displaced, and this also precluded the focused accumulation of significant melt volumes and the origin of large magmatic bodies. Nevertheless, judging from the occurrence of intrusions with layered structures, crystallizing differentiation in these bodies still has enough time to proceed. In the mobile environment, part of the still-liquid melt could be forced into other chambers and produce individual bodies, in which differentiation processes could continue. Consequently, numerous compositionally different small rootless intrusions that were formed at different depths within this belt were obviously prone to localize along the directions of the major stress field orientation during certain evolutionary episodes of the BMB.

A generalized model of Early Paleoproterozoic magmatic systems in the Baltic Shield beneath cratons and transitional intercratonic mobile belts, for example, BMB, is presented in Fig. 14.

CONCLUSIONS

(1) The Belomorian drusite (coronite) complex (2.46–2.36 Ga) consists of numerous small synkinematic mafic and ultramafic rootless intrusions widespread throughout the BMB area and metamorphosed to the amphibolite facies. Their volcanic analogues seem to be metavolcanic rocks (garnet amphibolites) of the Kandalaksha Formation and Tana Complex in Finland, which are exposed along the northern BMB margin.

(2) The intrusions can be subdivided into two major types. Type I comprises plagioclase lherzolites (*Ol* ± *Crt*, *Ol* + *Opx* ± *Crt*, and *Ol* + *Opx* + *Cpx* ± *Crt* cumulates), pyroxenites, melanocratic gabbronorites (*Opx* ± *Cpx* cumulates), olivine gabbronorites (*Ol* + *Opx* + *Pl* ± *Cpx* cumulates), and gabbronorites (*Opx* + *Pl* ± *Cpx* cumulates). Type II includes, along with norites and gabbronorites, abundant anorthosites and gabbronorite-anorthosites (*Pl* cumulates) and subordinate amounts of magnetite gabbro-diorites (*Opx* + *Pl* + *Cpx* + *Mag* cumulates).

(3) The composition and quantitative proportions of the rocks in the complex as a whole roughly correspond to those in large layered intrusions in the neighboring cratons. Both rock groups are similar in petrography, geochemistry, and isotopic geochemistry, which suggests that all of these rocks were produced by the same type of parental magmas: silicic high-Mg (boninite-like) series (SHMS). However, these rocks in the BMB display a clearly pronounced tendency toward forming individual bodies with the corresponding compositions of the inner-contact rocks.

(4) This complex was emplaced and then crystallized in a mobile environment, which caused the small sizes of the bodies and their wide distribution within the belt. Upon their solidification, the intrusions of the complex and their host gneisses and migmatites were involved in tectonic flowage processes under amphibolite-facies conditions at elevated pressures. As a result, most of the bodies have tectonized contacts, and their rocks were blastomylonitized and amphibolized. Relatively weakly altered rocks are preserved only in the central portions of the bodies and are characterized by widespread coronite (drusite) textures along the grain boundaries of primary magmatic minerals.

(5) The complex was produced not instantaneously but over a time span of approximately 100 m.y. There seems to be no correlations between the composition of the melts and the time of their emplacement. The spatial distribution of the bodies exhibits a clearly pronounced tendency toward their arrangement along the directions of the major stress fields during the major deformation episodes of the BMB in the Early Paleoproterozoic.

(6) The intrusions of the complex are components of the large Baltic SHMS province, whose genesis is thought to have been related to a mantle superplume of strongly depleted ultramafic material beneath the eastern part of the shield. The extension of the rigid cratonic crust above the laterally spreading head of the plume gave rise to graben-shaped volcano-sedimentary structures, dike swarms, and large layered intrusions. Areas adjacent to the zones of downgoing mantle flows were marked by the development of mobile belts (BMB and TLMB) with a dispersed type of their magmatism.

ACKNOWLEDGMENTS

The authors thank the Direction and the staff of the Kandalaksha Nature Reserve and V.Ya. Berger, the head of the Kartesh Biological Observatory of the Zoological Institute, Russian Academy of Sciences, for help during the fieldwork. The authors also thank S.P. Korikovsky, Corresponding member of the Russian Academy of Sciences, and Dr. O.A. Lukanin (Vernadsky Institute of Geochemistry and Analytical Chemistry, Russian Academy of Sciences), who reviewed the manuscript and expressed valuable remarks. This research was financially supported by the Russian Foundation for Basic Research (project nos. 01-05-64673 and 04-05-64581), the Federal Program for Support of Scientific Schools (Grant 1251.2003.5), and Program 5 of the Division for Earth Sciences of the Russian Academy of Sciences (contract no. 875).

REFERENCES

1. N. L. Alekseev, S. B. Lobach-Zhuchenko, E. S. Bogomolov, *et al.*, "Phase and Nd Isotopic Equilibria in Drusites of Cape Tolstik and the Tupaya Bay Area, Northwestern Belomorie, Baltic Shield," Petrologiya **7** (1), 3–23 (1999) [Petrology **7** (1), 1–20 (1999)].
2. N. L. Alexejev, T. F. Zinger, B. V. Belyatskii, and V. V. Balaganskii, "Age of Crystallization and Metamorphism of the Pezhostrov Gabbro–Anorthosites, Northern Karelia, Russia," *in Abstracts of Papers of SVEKALAPKO 5th Meeting* (Lammi, London, 2000), p. 3.
3. Yu. V. Amelin, L. M. Heaman, and V. S. Semenov, "U–Pb Geochronology of Layered Intrusions in the Eastern Baltic Shield: Implications for the Timing and Duration of Paleoproterozoic Continental Rifting," Precambrian Res. **75**, 31–46 (1995).
4. Yu. V. Amelin and V. S. Semenov, "Nd and Sr Isotope Geochemistry of Mafic Layered Intrusions in the Eastern Baltic Shield: Implications for the Sources and Contamination of Paleoproterozoic Continental Mafic Magmas," Contrib. Mineral. Petrol. **124**, 255–272 (1996).
5. V. V. Balaganskii, N. M. Kudryashov, Yu. V. Balashov, *et al.*, "The Age of the Zhemchuzhnyi Drusite Massif, Northwestern White Sea Area: U–Pb Isotopic Data and Geological Implications," Geokhimiya, No. 2, 158–168 (1997) [Geochem. Int. **35** (2), 127–136 (1997)].
6. P. Barbey and M. Raith, "The Granulite Belt of Lapland," in *Granulites and Crustal Evolution*, Ed. by D. Veilzent and Ph. Vidal (Kluwer, Dardrecht, 1990), pp. 111–132.
7. O. A. Belyaev and N. E. Kozlov, "Geology, Geochemistry, and Metamorphism of the Lapland Granulite Belt and Adjacent Areas in the Vuosto Area, Northern Finland," Geol. Surv. Finland. **138** (1997).
8. E. V. Bibikova, S. V. Bogdanova, V. A. Glebovitskii, *et al.*, "Evolution of the Belomorian Belt: NORDSIM U–Pb Zircon Dating of the Chupa Paragneisses, Magmatism, and Metamorphic Stages," Petrologiya **12** (3), 227–244 (2004) [Petrology **12** (3), 195–210 (2004)].
9. E. V. Bibikova, T. Shel'd, S. V. Bogdanova, *et al.*, "The Geochronology of Belomorides: Implication for Multistage Geological History," Geokhimiya, No. 10, 1393–1412 (1993).

10. S. V. Bogdanova, "High Grade Metamorphism of 2.45–2.4 Ga Age in Mafic Intrusions of the Belomorian Belt in the Northeastern Baltic Shield," in *Precambrian Crustal Evolution in the North Atlantic Region*, Ed. by T. S. Brewer, Geol. Soc. Spec. Publ., No. 112, 69–90 (1996).

11. A. V. Chistyakov, E. V. Sharkov, T. L. Grokhovskaya, *et al.*, "Petrology of the Europe-Largest Burakovsky Early Paleoproterozoic Layered Pluton, Southern Karelia, Russia," Russ. J. Earth Sci. **4** (1), (2002); http://rjes.wdcb.ru/.

12. M. M. Efimov, M. N. Bogdanova, and S. V. Bogdanova, "Periodicity and Types of Magmatism in the Archean of the Northwestern Belomorian Zone, Tolstik Area," in *Basic–Ultrabasic Magmatism of Main Structural–Lithologic Zones of Kola Peninsula* (Kol'sk. Nauchn. Tsentr, Ross. Akad. Nauk, Apatity, 1987), pp. 13–29 [in Russian].

13. T. V. Kaulina and N. M. Kudryashov, "The Evolution of the Belomorian Complex," in *Proceedings of the III All-Russian Conference 'General Problems in Precambrian Stratigraphy'* (Apatity, 2000), pp. 100–102 [in Russian].

14. E. K. Kozlov, B. A. Yudin, and V. S. Dokuchaeva, *Basic and Ultrabasic Complexes of Monche–Volch'i–Losevye Tundra* (Nauka, Leningrad, 1967) [in Russian].

15. T. L. Larikova, "Genesis of Drusitic (Coronitic) Textures around Olivine and Orthopyroxene during Metamorphism of Gabbroids in Northern Belomorie, Karelia," Petrologiya **8** (4), 430–448 (2000) [Petrology **8** (4), 384–400 (2000)].

16. S. B. Lobach-Zhuchenko, N. A. Arestova, V. P. Chekulaev, *et al.*, "Geochemistry and Petrology of 2.40–2.45 Ga Magmatic Rocks in the Northwestern Belomorian Belt, Fennoscandian Shield, Russia," Precambrian Res. **92**, 223–250 (1998).

17. N. D. Malov and E. V. Sharkov, "The Composition of Parental Melts and the Formation Conditions of the Belomorian Drusite Complex," Geokhimiya, No. 7, 1032–1039 (1978).

18. F. P. Mitrofanov and V. I. Pozhilenko, *The Voche-Lambina Archean Geodynamic Area in the Kola Peninsula* (Kol'sk. Nauchn. Tsentr, Akad. Nauk SSSR, Apatity, 1991) [in Russian].

19. B. J. Murton, D. W. Peete, R. J. Arculus, *et al.*, "Trace-Element Geochemistry of Volcanic Rocks from Site 786: The Izu–Bonin Forearc," in *Proceedings of ODP, Scientific Results, 125, College Station, TX (Ocean Drilling Program)*, Ed. by P. Fryer, J. A. Pearce, L. B. Stokking, *et al.* (London, 1992), pp. 211–236.

20. L. A. Priyatkina and E. V. Sharkov, *The Geology of the Lapland Deep Fault, Baltic Shield* (Nauka, Leningrad, 1979) [in Russian].

21. I. S. Puchtel, K. M. Haase, A. W. Hofmann, *et al.*, "Petrology and Geochemistry of Crustally Contaminated Komatiitic Basalts from the Vetreny Belt, Southeastern Baltic Shield: Evidence for an Early Proterozoic Mantle Plume beneath Rifted Archean Continental Lithosphere," Geochim. Cosmochim. Acta **61** (6), 1205–1222 (1997).

22. E. V. Sharkov and V. F. Smol'kin, "The Early Proterozoic Pechenga–Varzuga Belt: A Case of Precambrian Back-Arc Spreading," Precambrian Res. **82**, 133–151 (1997).

23. E. V. Sharkov, O. A. Bogatikov, and I. S. Krasivskaya, "The Role of Mantle Plumes in the Early Precambrian Tectonics of the Eastern Baltic Shield," Geotektonika, No. 2, 3–25 (2000) [Geotectonics **34** (2), 85–105 (2000)].

24. E. V. Sharkov, V. F. Smol'kin, A. V. Chistyakov, *et al.*, "The Geology and Metallogeny of the Monchegorsk Layered Complex," in *Russian Arctic: Geological Evolution, Metallogeny, and Geoecology* (VNIIOkeangeologiya, St. Petersburg, 2002), pp. 485–494 [in Russian].

25. E. V. Sharkov, V. F. Smol'kin, and I. S. Krasivskaya, "Early Proterozoic Igneous Province of Silicic High-Mg Boninite-like Rocks in the Eastern Baltic Shield," Petrologiya **5** (5), 503–522 (1997) [Petrology **5** (5), 448–465 (1997)].

26. E. V. Sharkov, Vl. V. Lyakhovich, and G. V. Ledneva, "The Petrology of the Belomorian Drusite Complex: Evidence from the Pezhostrov Massif," Petrologiya **2** (5), 511–531 (1994).

27. K. A. Shurkin, N. V. Gorlov, M. E. Sal'e, *et al.*, *The Belomorian Complex in Northern Karelia and Southwestern Kola Peninsula: Geology and Pegmatite-Bearing Potential* (Akad. Nauk SSSR, Moscow, 1962) [in Russian].

28. A. I. Slabunov, A. N. Larionov, E. V. Bibikova, *et al.*, *The Geology and Geochronology of the Shobozero Lherzolite–Gabbronorite Pluton, the Belomorian Mobile Belt*, Ed. by A. I. Golubev and V. V. Shchiptsov (Karel. Nauchn. Tsentr, Ross. Akad. Nauk, Petrozavodsk, 2001), Vol. 3, pp. 3–14 [in Russian].

29. V. S. Stepanov, *Precambrian Basic Magmatism in the Western Belomorian Area* (Nauka, Leningrad, 1981) [in Russian].

30. O. I. Volodichev, *The Belomorian Rock Complex in Karelia: Geology and Petrology* (Nauka, Leningrad, 1990) [in Russian].

31. T. F. Zinger, J. Gotze, O. A. Levchenkov, *et al.*, "Zircon in Polydeformed and Metamorphosed Precambrian Granitoids from the White Sea Tectonic Zone, Russia: Morphology, Cathodoluminescence, and U–Pb Chronology," Int. Geol. Rev. **38**, 57–73 (1996).